Pilot Study on Geometrical Measurement of the Rockwell Diamond Indenter

Final Report – 08 October 2019

Pilot Study on

Geometrical Measurement of the Rockwell Diamond Indenter

CIPM / CCM / WORKING GROUP ON HARDNESS

Pilot Study code: CCM.H-P1

Pilot Laboratory: INMETRO / BRAZIL

NMI PARTICIPANTS:

INMETRO/Brazil; NIST/USA; INRiM/Italy; PTB/Germany; TUBITAK UME/Turkey; KRISS/South Korea; VNIIFTRI/Russia; NIMT/Thailand; NIM/PR China

CO-AUTHORS:

Renato Reis Machado (INMETRO/Brazil); Samuel Low (NIST/USA); Alessandro Germak (INRiM/Italy); Febo Menelao (PTB/Germany); Cihan Kuzu (TUBITAK UME/Turkey); Nae Hyung Tak (KRISS/South Korea); Edward Aslanyan (VNIIFTRI/Russia); Sanponpute Tassanai (NIMT/Thailand); Cui Yuanyuan (NIM/PR China)

Contents

Nomenclature

BIPM	International Bureau of Weights and Measures
CC	Consultative Committee
CCM	Consultative Committee for Mass and Related Quantities
CIPM	International Committee for Weights and Measures
INMETRO	National Institute of Metrology, Quality and Technology
INRiM	National Institute for Metrological Research
ISO	International Standards Organization
KCDB	Key Comparison Data Base
KRISS	Korean Research Institute of Standard and Science
NIM	National Institute of Metrology of China
NIMT	National Institute of Metrology of Thailand
NIST	National Institute of Standards and Technology
PTB	National Metrology Institute of Germany
RM	Reference Material
SI	International System of Units
TUBITAK UME	National Metrology Institute of Turkey
VNIIFTRI	Russian National Scientific and Research Institute for Physical, Technical and Radiotechnical Measurements
NMIJ	National Metrology Institute of Japan
NPL	National Physical Laboratory

1. Foreword

This report describes a CCM Pilot Study conducted by the CCM/Working Group on Hardness of systems used to calibrate the diamond geometry of Rockwell Diamond Indenters.

2. Background to the comparison

There have been numerous discussions among the members of the CCM Working Group on Hardness (WGH) concerning the difficulty in obtaining calibration-grade Rockwell hardness diamond indenters having the correct shape within geometric tolerances as specified in international test method standards. There are two main reasons for this difficulty. The primary reason is that the crystallographic structure of diamond makes it extremely difficult to grind and polish a diamond to the required Rockwell indenter shape. The Rockwell indenter shape is a cone having a 120 ° included angle and a spherical tip radius of 0,2 mm. Secondly, the accurate measurement of a Rockwell indenter's geometrical parameters is also a difficult and often time-consuming process due to the conical and spherical indenter geometries and the optical transparency and high reflectivity of the polished diamond.

During the 8th meeting of the WGH on September 16-21, 2006 in Rio de Janeiro, Brazil, it was agreed to carry out a Pilot Study on the measurement of Rockwell hardness diamond indenters in which the hardness and/or dimensional metrology laboratories of National Metrology Institutes (NMIs) should participate.

The objective of this study was to compare the systems being used to characterize the indenter geometry, by measuring the included angle, the straightness of the generatrix, the tip radius, the deviation of the local radius and the tilt.

3. Participants in the comparison

The National Metrology Institute of Quality and Technology (INMETRO/Brazil) agreed to act as the pilot laboratory for this comparison study, and has carried out the development of the test protocol and the planning of the comparisons, initially, between ten participating laboratories. However, during the work of comparison, some laboratories asked to be withdraw, which were the cases of the NMIJ/Japan and NPL/UK and other asked to be added, which was the case of the NIMT/Thailand, occurred after the 13th meeting of the CCM/WGH held at the BIPM. Thereby, this report reflect the comparison among the nine NMI listed in Table 1.

Table 1: Participating NMI code and the comparison schedule

NMI/Country	NMI code	Test Date
INMETRO/Brazil	A	December 2010
NIST/USA	B	January 2011
INRiM/Italy	D	April 2011
PTB/Germany	E	June 2011
TUBITAK UME/Turkey	F	July 2011
KRISS/South Korea	G	August 2011
VNIIFTRI/Russia	H	October 2011
NIMT/Thailand	I	January 2013
NIM/PR China	J	March 2013
INMETRO/Brazil	A	January 2015

4. Principles of the comparison

The purpose of this CCM-Pilot Study was to explore and to know how the National Metrology Laboratories (NMIs) are measuring, analyzing and reporting their results of the Rockwell diamond indenter geometry calibrations. This study intended to be the first exercise of the NMIs, before the realization of a CCM-Key Comparison that should establish the best measurement capability of national laboratories that are engaged in the metrological characterization of these diamond indenters.

Three Rockwell diamond indenters were chosen as test artifacts. They were circulated among the laboratories with the following characteristics: one indenter with a near-nominal shape and the other two indenters with geometric parameters near to the permissible limits as defined by the international standard ISO 6508 Part 3 [1]. Figure 1 gives the approximate overall dimensions of the indenters.

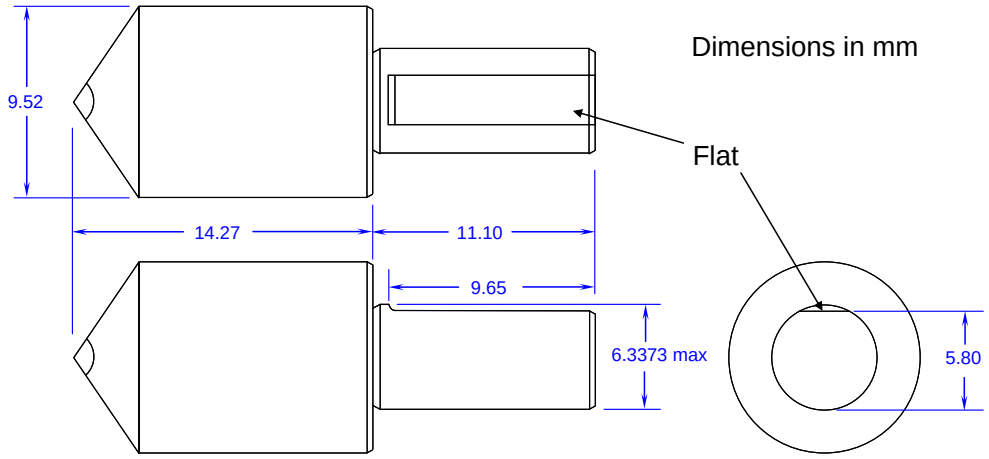

Figure 1: Approximate dimensions of the indenters

5. Procedure

5.1. Test artifacts (measurand)

In this Pilot Study, three Rockwell hardness diamond indenters designated as indenters 104, 122 and 130 (as engraved on each indenter) were measured for specific geometry parameters by the participating laboratories.

These three indenters were provided by the National Institute of Standards and Technology (NIST/USA). They were chosen for the pilot laboratory from an inventory of 28 indenters previously measured by NIST.

5.2. Format of the comparison

The participating laboratories of this Pilot Study conducted dimensional measurements of specified geometric parameters on each of the three Rockwell diamond indenters using their usual procedures for qualifying them, and according to the capacity of their measurement systems. Those laboratories that did not have their own procedures to qualify Rockwell diamond indenters were instructed to follow the requirements defined in ISO 6508 Part 3 [1]. Deviations from the procedures established in this standard were to be reported.

The dimensional measurements were intended to illustrate measurement biases among NMIs and measurement differences between different types of measuring instruments. The pilot laboratory made measurements at the beginning and at the end of the pilot study comparison in order to evaluate the stability of the indenters. The geometrical parameters measured were the following (Figure 2), according to ISO 6508-3:2005 [1] clause 4.5 (*a* through *c*):

- Included cone angle of the diamond (θ).
- Radius of the spherical tip of the diamond (*r*).
- Profile deviation of the local radius from the least square mean radius value.
- Straightness of the generatrix of the diamond cone, adjacent to the blend of the spherical and conical parts, over length of 0,4 mm.
- Angle between the axis of the diamond cone and the axis normal to the seating surface.

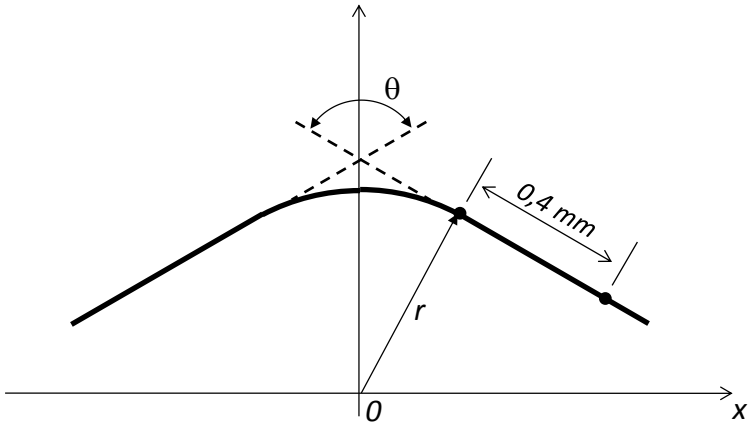

Figure 2: Illustration of the geometries of the Rockwell diamond

The diamond indenter had to be inspected by an optical microscope with at least 400x of magnification before and after the measurements for each NMI participant.

5.3. Indenter calibration systems

The Rockwell diamond indenter calibration system should be capable of making the dimensional measurements specified in ISO 6508-3:2005 [1] clause 4.5 (*a* through *c*).

Before conducting any measurements, each NMI participant carried out the calibration of the measurement instruments and, consequently, determined the measurement uncertainties.

For measurement systems that make axial-plane measurements, if possible, the diamond shape measurements should be made at the 8 section locations, as illustrated in Figure 3 and described in Table 2. Measurement position 1 is in the axial plane of the indenter that is parallel with the flat on the indenter shaft. Position 2 is in the axial plane rotated 45 ° clockwise around the indenter axis from position 1 as the indenter tip points towards the operator. The remaining 6 measurements should be made similarly at 45 ° rotations.

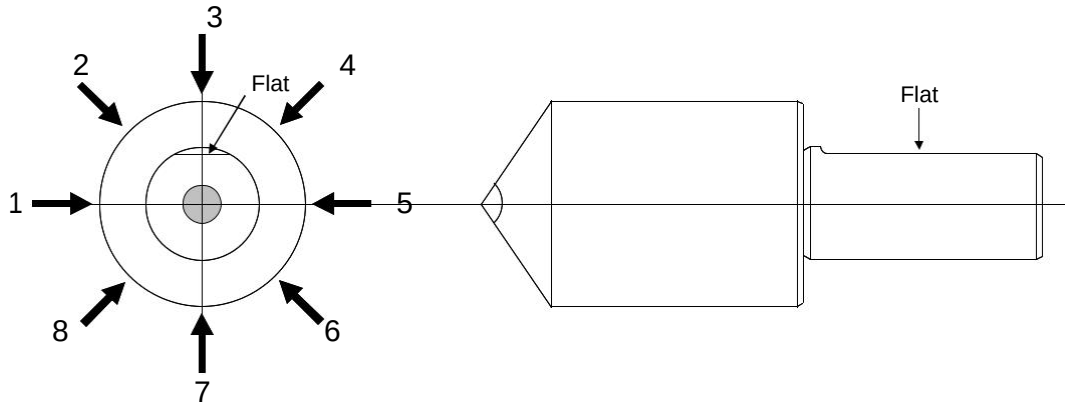

Figure 3: Illustration of the measurement sections of a Rockwell diamond indenter. The figure on the left is oriented with diamond tip pointing towards to the operator [2].

Table 2: Measurement sections of Rockwell diamond indenters (8 positions at 45 ° intervals)

Section Number	Section Location
1	0 °
2	45 °
3	90 °
4	135 °
5	180 °
6	225 °
7	270 °
8	315 °

6. Transportation

The set of indenters was sent from one participant to the next participant following the schedule given in Table 1. The indenters were stored and shipped in the supplied black plastic transport case as shown in Figure 4. Each participating Institute assumed the costs for customs to receive the indenters and for the transport and related administrative fees associated with sending the indenters to the next NMI participant.

Upon receipt of the indenters at each laboratory, the indenters were inspected for damage.

Prior to shipping the indenters to the next NMI participant, the indenters were cleaned with alcohol (ethanol) and packed in the shipping box (Figure 4). Immediately after shipping the indenters, the next NMI participant and the pilot laboratory were notified by email about this stage.

Figure 4: Shipping container with three indenters

7. Data report

Each NMI participant reported the following information on the supplied data sheet.

a) A short description of the hardness indenter calibration systems used in the laboratory for the measurements, including the measurement principle(s) and the name of the manufacturer(s) of the measuring system.

b) The results of the geometric measurements of the three travelling indenters: #104, #122, and #130.

c) The declared uncertainty of the measurements.

NOTE: The measurement uncertainty should be estimated according to the annexes of the ISO 6508 Part 2 [3] and Part 3 [1], the ISO GUM [4] and the EURAMET/cg-16 [5].

d) Deviations from this technical protocol and/or from the reference documents.

8. Description of the indenter calibration systems

8.1 INMETRO/Brazil

The Gal-Indent system used to run the measurements of the diamond indenter is manufactured by LTF S.p.a., Italy. The Gal-Indent operates using two independent systems. The cone angle is measured using the sine-bar device, and the tip radius is measured using the rotary table.

8.1.a) Included cone angle of the diamond

The sine-bar device is used to measure the angle between the faces, the straightness, and the orthogonality of the cone. The microscope attached to the system has a metrological amplifier and two interferometry object-glasses, where the light beam is divided in two beams. One is reflected over the observed surface and the other goes directly to the field of observation of the CCD camera. The two beams initially separated, are recomposed to form an interference pattern with bright and dark fringes.

Using this physical measurement technique, it is possible to reconstruct the geometry of an observed surface by the interferometry fringes that are formed. These fringes represent the local geometry of the normal axis to the optical axis.

8.1.b) Radius of the spherical tip of the diamond

The rotary table is used to characterize the spherical tip of the Rockwell diamond indenter. It works by rotating the indenter in a stationary axis to detect its profile displacement through a Linear Variable Displacement Transducer (LVDT) which has a spherical tip. The measurement system is calibrated against a reference ruby sphere with a 200 µm radius. The ruby sphere is used to zero the system. The mean radius of the indenter tip is determined by measuring the indenter tip radius 8 times.

8.2 NIST/USA

The Rockwell diamond indenters are measured at NIST with a microform calibration system which consists of a commercial stylus instrument – Form Talysurf manufactured by the Taylor Hobson Inc. in the United Kingdom, an x-y stage and a rotary stage, a set of calibration and check standards, and a calibration and uncertainty procedure.

The stylus instrument uses a stylus-laser sensor with 0.0008 µm vertical digital resolution and ± 6 mm range, and 0.125 µm horizontal digital resolution and 200 mm range. The nominal stylus radius is 2 µm. The nominal stylus contact force is 100 mgf (≈ 0.001 N). An x-y stage and a rotary stage combined with a specially designed indenter holder are used for the alignment of the Rockwell diamond indenters. Both the holder geometric axis and the rotation axis of the rotary stage are aligned relative to the instrument z-axis.

8.2.a) Radius of the spherical tip of the diamond and the Profile deviation of the local radius from the least square mean radius value.

It was used a stylus traces with 1,2 mm (or ± 0,6 mm) length across the radius tip of the indenter, in which 9600 data points were collected.

By windowing on the central ± 100 µm part of the trace (Figure 5) and using a least squares arc fitting algorithm, the least squares radius and profile deviation from the fitted radius were determined.

8.2.b) Included cone angle of the diamond and the Straightness of the generatrix of the diamond cone.

By windowing on the remaining left and right portions of the trace, located from - 450 µm to - 100 µm on the left and from + 100 µm to + 450 µm on the right (Figure 3), and using the least squares line fitting algorithm, the indenter cone angle and cone flank straightness error were determined.

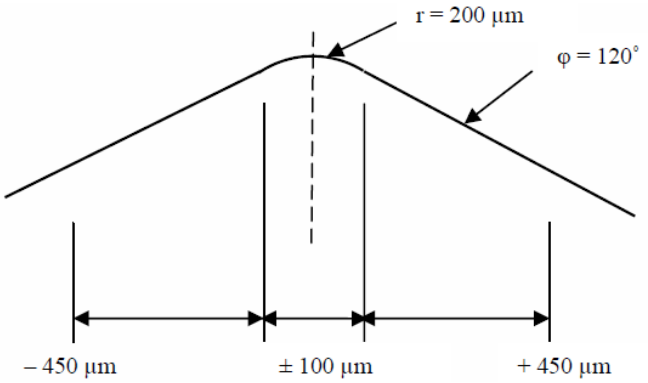

Figure 5: Three windows for data fitting of tip radius and profile deviation at ± 100 µm of the center the cone angle and the cone flank straightness fitting at ± (100 to 450) µm [6]

8.3 INRiM/Italy

The diamond indenter geometry measurement system was developed and realized in INRiM (and subsequently commercialized by LTF S.p.a.-Italy as Gal-vision system).

8.1.a) Included cone angle of the diamond

For the angle measurement, the system uses a tilting table with an angle measuring system (encoder). An interferometric microscope is used as a collimation system in order to detect the parallel position between the optical system (based on an interferometric lenses) and the surface of the indenter using a fringe pattern recognition, for two opposite generatrix of the cone.

8.1.b) Radius of the spherical tip of the diamond

To measure the roundness of the tip, a contact comparator system is used. It is made up of a rotating table on an air bearing (high stiffness) and a linear transducer to compare the radius of a ruby sphere, used as a reference, to those spherical of the indenter.

NOTE: The declared expanded uncertainty and best measurement capability are related only to the single section measurement (measurement value). The expanded uncertainty of the final mean value (119,95 °) is 0,025 ° and the best measurement capability of the system when it measures the mean value is 0,022 °.

8.4 PTB/Germany

8.4.a) Radius of the spherical tip of the diamond

The tip radius measurement system used was a non-imaging PTB self-made system based on a confocal (position)-sensing method [7].

8.4.b) Included cone angle of the diamond

The angle measurement system used was a PTB self-made system based on optical interference microscope that gives an indication of when the surface of the indenter is in a horizontal position. After this, the indenter is rotated to the opposite surface. Again, the microscope gives an indication about the horizontal position. The

movement angle is measured. The angle of the indenter is then 180 ° minus the movement angle.

NOTE: The system gives a mean value of the complete top surface of the indenter. It is not possible to separate it to different angles.

8.5 TUBITAK UME/TURKEY

The systems used for the geometrical verification/calibration of the diamond indenters for Rockwell, Rockwell superficial, Vickers and MicroVickers indenters were the Gal-vision and the Rotary table, both systems manufactured by LTF S.p.a., Italy. The Gal-vision system consists of an interferometric sine-bar, for angular, straightness and flatness measurement. The Rotating table system was used for the verification of the spherical tip of Rockwell indenters. The two instruments are set up in one workstation, interfaced with the same computer for data analysis.

NOTE 1: The profile deviation is not distinguished valley or peak. It is considered mixed as just deviation and written in the peak column.

NOTE 2: In the calibration of tilt between the diamond cone and the normal to the seating surface, the measurement is not done in one particular position. It is a combined tilt measurement after completing the whole cycle. And the measurement is made indeed between the axis of the diamond cone and the axis of the indenter holder, but could be accepted as requested, between the diamond cone and the normal to the seating surface.

8.6. KRISS/SOUTH KOREA

8.6.a) Radius of the spherical tip of the diamond, Included cone angle of the diamond and the Profile deviation of the local radius from the least square mean radius value.

The 1st measurement system: it was used a 3D dimensional laser confocal microscope.

Manufacturer: OLYMPUS, Japan
Model: LEXT OLS4100

The 2nd measurement system: a CNC video measuring system was used.

Manufacturer: NIKON, Japan
Model: NEXIV VMH-300N

NOTES: 1) The measured value is obtained by the 2nd measurement system.
2) The measured value was chosen to be the largest value among the measured values at each position of the indenter axis.

8.7 VNIIFTRI/RUSSIA

8.7.a) Radius of the spherical tip of the diamond, Included cone angle of the diamond and the Profile deviation of the local radius from the least square mean radius value.

Hardness measuring laboratory VNIIFTRI used the system GAL-INDENT for measuring geometrical parameters of Rockwell indenters. GAL-INDENT was manufactured by LTF S.p.a., Italy and consists of interferometry Sine Bar and Rotary Table.

The Sine Bar is based on Mirau interferometry for the measurement of angles, straightness, angle between the axis of the diamond cone and the axis normal to the seating surface. The Rotary table is used to measure the radius of the spherical tip of the Rockwell cone indenter.

The Rotary table is adopted to rotate the indenter around the center of the nominal radius and detecting the displacement of the actual profile from the reference by a linear transducer with a spherical probe. By repeating this operation in several axial sections of the indenter, the full geometry of the tip can be reconstructed to give a global evaluation of the tip itself.

8.8 NIMT/THAILAND

8.8.a) Radius of the spherical tip and included cone angle of the diamond

In calibration of tip radius and cone angle, the cross-section profile of each plane of indenter was measured by a surface-roughness measuring machine, SV-3100 made by Mitutoyo. The instrument was operated in contour mode. In order to find the tip position, the indenter was manually scanned in steps of 5 μm. Some correction of stylus was added by using a set of pin gauge as a standard.

8.9 NIM/China

8.9.a) Radius of the spherical tip of the diamond and Included cone angle of the diamond

The measuring instruments used were a multi sensor coordinate measurement machine with a confocal sensor for 3D measurement of the indenter shape, made by Werth Messtechnik GmbH, Germany.

9. Reference values

Even not being the main focus of this study, it was established the following parameters as reference for every measure performed, in accordance with the ISO standard [1].

- Included cone angle of the diamond.

  Reference: mean included angle of (120 ± 0,1) °.

- Radius of the spherical tip of the diamond.

  Reference: mean radius of (0,200 ± 0,005) mm.

- Profile deviation of the local radius from the least square mean radius value.

  Reference: within 0,002 mm

- Straightness of the generatrix of the diamond cone, adjacent to the blend of the spherical and conical parts.

  Reference: not exceed 0,000 5 mm over a minimum length of 0,4 mm.

- Angle between the axis of the diamond cone and the axis normal to the seating surface.

  Reference: within 0,3 °.

10. Method of analysis

10.1 Weighted mean method

One of the method used to analyze the results of the comparison, and to determine the dispersion of the obtained data points by the Labs was the *weighted mean method*, Equation 1.

$$\overline{w} = \frac{\sum_i^n x_i \times w_i}{\sum_i^n w_i} \quad (1)$$

where

$\overline{w}$ weighted mean

x_i measured values provided by the NMI participant

w_i weight

$$w_i = \frac{1}{{u_i}^2} \quad (2)$$

where

u_i standard uncertainty from weight

From the above method of analysis, the normalized errors from the weighted mean (*E*n.w), Equation 4, were then calculated, and the respective graphics were plotted (clause 11.4).

$$En.w = \frac{(\mathrm{x}_i - \overline{w})}{\sqrt{{\mathrm{U}_i}^2 - {\mathrm{U}_{ref}}^2}} \quad (3)$$

where

$En.w$ normalized error form the weighted mean

x_i measured values provided by the NMI participants

$\overline{w}$ weighted mean value

U_i expanded uncertainty provided by the NMI participants

U_{ref} reference value of the expanded uncertainty from weight

10.2 Possolo weighted mean method

The other method used to analyze the results of the comparison, and to determine the dispersion of the obtained data points by the Labs was the method based on the "NIST Consensus Builder (NICOB)" methodology, which is calling in this work as *Possolo weighted mean method*. This method consistent with the combination of measurement results obtained independently by different laboratories or measurement methods [8, 9].

Among the three procedures available in the NICOB, the DerSimonian-Laird was the procedure applied to this analysis. This procedure uses as a weighted mean the Equation (4).

$$\overline{w}_p = \frac{\sum_i^n x_i \times w_{i.p}}{\sum_i^n w_{i.p}} \quad (4)$$

where

$\bar{w}_p$ Possolo weighted mean

x_i measured values provided by the NMI participant

$w_{i.p}$ Possolo weight

$$w_{i.p} = \frac{1}{u_i^2 + \tau^2} \quad (5)$$

where

u_i^2 uncertainty associated with the value measured by the NMIs

τ^2 indication of the heterogeneity of the measured results

From the above method of analysis, the normalized errors from the Possolo weighted mean (*E*n.p), Equation 6, were then calculated, and the respective graphics were plotted (clause 11.4).

$$En.p = \frac{(x_i - \bar{w}_p)}{\sqrt{U_i^2 - U_{ref}^2}} \quad (6)$$

where

$En.p$ normalized error from Possolo weighted mean

x_i measured values provided by the NMI participants

$\bar{w}_p$ Possolo weighted mean value

U_i expanded uncertainty provided by the NMI participants

U_{ref} reference value of the expanded uncertainty from Possolo weight

11. General results and discussions

11.1 Table results of the measurements performed by the NMI participants

The measurement matrix for the Rockwell hardness diamond indenters performed by each of the NMI participants for the pilot study is provided in Table 3 to Table 11. All measurements were to be performed at room temperature (22 ± 2) °C.

NOTE 1: The results obtained for the dimensional measurements of the indenters were entered on the document (*Indenter pilot study_data sheet.xls*), provided by the pilot laboratory with the technical protocol.

It is important to point out that some NMIs did not provide all set of parameters listed on the pilot indenter protocol. It may be due to the indenter calibration systems restrictions.

Some NMIs provided their results considering several measurement windows. Consequently, for each window, different values were obtained for the same indenter. The windows considered in this report, were those around the window values described by John Song *et all* [10]. They said that for an ideally shaped Rockwell indenter, as specified in the standards [11] and [1], i.e., 200 µm tip radius blending with a 120 ° cone angle in a true tangential manner, the window sizes must be ± 100 µm for the tip radius calibration; and ± (100 to 450) µm along the x-axis for the left and right contributions to the cone angle calibration, and the sizes must be specified in the data analysis.

This is especially important for calculation of least squares radius and profile deviation in the center and cone flank straightness in the left and right. Furthermore, the blend area of the tip radius and cone angle must be accounted for when choosing window positions. Beyond these considerations, John Song *et all* [10], said that the blend point can vary position depending on the actual cone angle and tip radius. In the light of these deviations, on the transition area between the radial tip surface and the linear cone surface, both the ASTM and ISO standards specify that the straightness of the cone flank is measured “adjacent to the blend” which leaves some flexibility in the choice of the size and position of the windows on the flanks.

Table 3: General results of INMETRO/Brazil measurements (code A)

Parameters	**HRC Indenter #**		
	104	122	130
	NMI mean value / NMI expanded uncertainty		
Included cone angle (°)	120,02 / 0,06	120,04 / 0,05	119,99 / 0,05
Radius of the spherical tip (µm)	199,39 / 1,70	205,14 / 1,65	205,80 / 1,70
Max profile deviation of the local radius from the least square mean radius value (µm)	not informed	not informed	not informed
Straightness of the generatrix of the diamond cone (µm)	0,30 / 0,20	0,30 / 0,15	0,30 / 0,15
Angle between the axis of the diamond cone and the axis normal to the seating surface (°)	0,062 / 0,04	0,033 / 0,04	0,050 / 0,04

Table 4: General results of NIST/USA measurements (code B)

Parameters	HRC Indenter #		
	104	122	130
	NMI mean value / NMI expanded uncertainty		
Included cone angle (°)	119,94 / 0,01	119,99 / 0,01	120,03 / 0,02
Radius of the spherical tip (µm)	197,59 / 0,89	201,64 / 0,91	204,51 / 0,67
Max profile deviation of the local radius from the least square mean radius value (µm)	0,63 / 0,10	0,05 / 0,10	0,30 / 0,10
Straightness of the generatrix of the diamond cone (µm)	0,91 / 0,05	1,10 / 0,05	0,87 / 0,05
Angle between the axis of the diamond cone and the axis normal to the seating surface (°)	0,09 / 0,03	0,26 / 0,04	0,18 / 0,03

Table 5: General results of INRiM/Italy measurements (code D)

Parameters	HRC Indenter #		
	104	122	130
	NMI mean value / NMI expanded uncertainty		
Included cone angle (°)	119,95 / 0,03	120,01 / 0,03	120,05 / 0,03
Radius of the spherical tip (µm)	197,95 / 0,85	201,60 / 0,71	203,53 / 0,63
Max profile deviation of the local radius from the least square mean radius value (µm)	not informed	not informed	not informed
Straightness of the generatrix of the diamond cone (µm)	0,30 / 0,15	0,30 / 0,15	0,30 / 0,15
Angle between the axis of the diamond cone and the axis normal to the seating surface (°)	0,08 / 0,05	0,13 / 0,05	0,09 / 0,05

Table 6: General results of PTB/Germany measurements (code E)

Parameters	HRC Indenter #		
	104	122	130
	NMI mean value / NMI expanded uncertainty		
Included cone angle (°)	119,99 / 0,04	120,00 / 0,04	119,93 / 0,04
Radius of the spherical tip (µm)	199,90 / 5,20	200,60 / 2,10	208,20 / 3,80
Max profile deviation of the local radius from the least square mean radius value (µm)	not informed	not informed	not informed
Straightness of the generatrix of the diamond cone (µm)	not informed	not informed	not informed
Angle between the axis of the diamond cone and the axis normal to the seating surface (°)	0,01 / 0,04	0,01 / 0,04	0,03 / 0,04

Table 7: General results of TUBITAK UME/Turkey measurements (code F)

Parameters	HRC Indenter #		
	104	122	130
	NMI mean value / NMI expanded uncertainty		
Included cone angle (°)	119,94 / 0,07	120,0 / 0,05	120,09 / 0,08
Radius of the spherical tip (µm)	200,38 / 2,00	205,53 / 2,60	206,80 / 2,06
Max profile deviation of the local radius from the least square mean radius value (µm)	1,86 / 0,95	2,06 / 0,82	1,46 / 1,07
Straightness of the generatrix of the diamond cone (µm)	0,31 / 0,22	0,32 / 0,22	0,51 / 0,22
Angle between the axis of the diamond cone and the axis normal to the seating surface (°)	0,05 / 0,06	0,14 / 0,06	0,12 / 0,06

Table 8: General results of KRISS/South Korea measurements (code G)

Parameters	HRC Indenter #		
	104	122	130
	NMI mean value / NMI expanded uncertainty		
Included cone angle (°)	119,86 / 0,04	119,89 / 0,04	119,96 / 0,04
Radius of the spherical tip (µm)	199,80 / 1,50	202,70 / 1,50	205,80 / 1,50
Max profile deviation of the local radius from the least square mean radius value (µm)	0,70 / 0,50	0,60 / 0,50	0,30 / 0,50
Straightness of the generatrix of the diamond cone (µm)	1,00 / 0,50	0,70 / 0,50	1,00 / 0,50
Angle between the axis of the diamond cone and the axis normal to the seating surface (°)	0,60 / 0,05	0,51 / 0,05	0,53 / 0,05

Table 9: General results of VNIIFTRI/Russia measurements (code H)

Parameters	HRC Indenter #		
	104	122	130
	NMI mean value / NMI expanded uncertainty		
Included cone angle (°)	120,01 / 0,04	120,04 / 0,06	120,10 / 0,04
Radius of the spherical tip (µm)	198,13 / 1,80	202,40 / 1,60	204,50 / 1,60
Max profile deviation of the local radius from the least square mean radius value (µm)	0,30 / 0,20	0,40 / 0,40	0,50 / 0,40
Straightness of the generatrix of the diamond cone (µm)	0,18 / 0,14	0,17 / 0,14	0,46 / 0,28
Angle between the axis of the diamond cone and the axis normal to the seating surface (°)	0,06 / 0,02	0,09 / 0,02	0,05 / 0,02

Table 10: General results of NIMT/Thailand measurements (code I)

Parameters	HRC Indenter #		
	104	122	130
	NMI mean value / NMI expanded uncertainty		
Included cone angle (°)	120,05 / 0,05	120,00 / 0,05	120,01 / 0,05
Radius of the spherical tip (µm)	198,50 / 1,00	202,60 / 1,10	206,20 / 1,10
Max profile deviation of the local radius from the least square mean radius value (µm)	not informed	not informed	not informed
Straightness of the generatrix of the diamond cone (µm)	not informed	not informed	not informed
Angle between the axis of the diamond cone and the axis normal to the seating surface (°)	not informed	not informed	not informed

Table 11: General results of NIM/China measurements (code J)

Parameters	HRC Indenter #		
	104	122	130
	NMI mean value / NMI expanded uncertainty		
Included cone angle (°)	119,91 / 0,11	119,95 / 0,11	119,97 / 0,11
Radius of the spherical tip (µm)	198,80 / 1,50	201,90 / 1,50	208,70 / 1,50
Max profile deviation of the local radius from the least square mean radius value (µm)	1,10 / 1,00	1,10 / 1,00	1,10 / 1,00
Straightness of the generatrix of the diamond cone (µm)	1,50 / 1,00	1,2 / 1,0	1,80 / 1,00
Angle between the axis of the diamond cone and the axis normal to the seating surface (°)	0,11 / 0,01	0,14 / 0,08	0,14 / 0,08

11.2 Table results of the mean values and the normalized errors (*E*n) calculated for the NMI participants

From Table 12 to Table 26, it is possible to see the mean values measured by the NMI participants, their respective expanded uncertainties matrix and the normalized errors, *E*n.w and *E*n.p, related to the geometric parameters established on the pilot study protocol. It is important to point out that the *E*n values were determined by considering two methods of analysis. One from the weighted mean method, *E*n.w (see clause 10.1), and other form the Possolo weighted mean method, *E*n.p (see clause 10.2). The Tables 27 and 28 shows the calculated values related to the *weighted mean* and *Possolo weighted mean* method respectively.

11.2.1 Results of mean, expanded uncertainty and *E*n of cone angle

Table 12: Measurements of the *included cone angle of the diamond* related to the *indenter #104*.

Country	NMI code	NMI mean value (°)	NMI exp. unc. (°)	*E*n.w	*E*n.p
Brazil	A	120,02	0,06	1,34	0,87
USA	B	119,94	0,01	-0,68	-0,80
Italy	D	119,95	0,03	0,18	-0,33
Germany	E	119,99	0,04	0,99	0,44
Turkey	F	119,94	0,07	-0,075	-0,31
South Korea	G	119,86	0,04	-2,08	-1,98
Russia	H	120,01	0,04	1,58	0,88
Thailand	I	120,05	0,05	1,91	1,35
China	J	119,91	0,11	-0,32	-0,47

Table 13: Measurements of the *included cone angle of the diamond* related to the *indenter #122*.

Country	NMI code	NMI mean value (°)	NMI exp. unc. (°)	*E*n.w	*E*n.p
Brazil	A	120,04	0,05	1,01	0,86
USA	B	119,99	0,01	-0,15	-0,15
Italy	D	120,01	0,03	0,74	0,48
Germany	E	120,00	0,04	0,15	0,09
Turkey	F	120,00	0,05	0,20	0,14
South Korea	G	119,89	0,04	-2,42	-2,09
Russia	H	120,04	0,06	0,82	0,72
Thailand	I	120,00	0,05	0,26	0,20
China	J	119,95	0,11	-0,36	-0,37

Table 14: Measurements of the *included cone angle of the diamond* related to the *indenter #130*.

Country	NMI code	NMI mean value (°)	NMI exp. unc. (°)	*E*n.w	*E*n.p
Brazil	A	119,99	0,05	-0,70	-0,43
USA	B	120,03	0,02	0,34	0,43
Italy	D	120,05	0,03	0,89	0,80
Germany	E	119,93	0,04	-2,17	-1,55
Turkey	F	120,09	0,08	0,77	0,82
South Korea	G	119,96	0,04	-1,56	-1,03
Russia	H	120,10	0,04	1,81	1,60
Thailand	I	120,01	0,05	-0,30	-0,11
China	J	119,97	0,11	-0,49	-0,39

11.2.2 Results of mean, expanded uncertainty and *E*n of radius of the spherical tip

Table 15: Measurements of the *radius of the spherical tip of the diamond* related to the *indenter #104*.

Country	NMI code	NMI mean value (µm)	NMI exp. unc. (µm)	*E*n.w	*E*n.p
Brazil	A	199,39	1,70	0,56	0,43
USA	B	197,59	0,89	-0,83	-0,93
Italy	D	197,95	0,85	-0,48	-0,62
Germany	E	199,90	5,20	0,29	0,25
Turkey	F	200,38	2,00	0,96	0,85
South Korea	G	199,80	1,50	0,89	0,73
Russia	H	198,13	1,80	-0,15	-0,25
Thailand	I	198,50	1,00	0,08	-0,09
China	J	198,80	1,50	0,25	0,12

Table 16: Measurements of the *radius of the spherical tip of the diamond* related to the *indenter #122*.

Country	NMI code	NMI mean value (µm)	NMI exp. unc. (µm)	*E*n.w	*E*n.p
Brazil	A	205,14	1,65	1,75	1,43
USA	B	201,64	0,91	-0,53	-0,70
Italy	D	201,60	0,71	-0,70	-0,83
Germany	E	200,60	2,10	-0,74	-0,84
Turkey	F	205,53	2,60	1,28	1,12
South Korea	G	202,70	1,50	0,34	0,11
Russia	H	202,40	1,60	0,14	-0,06
Thailand	I	202,60	1,10	0,36	0,07
China	J	201,90	1,50	-0,18	-0,35

Table 17: Measurements of the *radius of the spherical tip of the diamond* related to the *indenter #130*.

Country	NMI code	NMI mean value (µm)	NMI exp. unc. (µm)	*E*n.w	*E*n.p
Brazil	A	205,80	1,70	0,54	0,01
USA	B	204,51	0,67	-0,45	-0,98
Italy	D	203,53	0,63	-1,82	-1,76
Germany	E	208,20	3,80	0,88	0,61
Turkey	F	206,79	2,06	0,93	0,43
South Korea	G	205,80	1,50	0,61	0,01
Russia	H	204,50	1,60	-0,22	-0,66
Thailand	I	206,20	1,10	1,16	0,27
China	J	208,70	1,50	2,49	1,56

11.2.3 Results of mean, expanded uncertainty and *E*n of max profile deviation

Table 18: Measurements of the *max profile deviation of the local radius from the least square mean radius value* related to the *indenter #104*.

Country	NMI code	NMI mean value (µm)	NMI exp. unc. (µm)	*E*n.w	*E*n.p
USA	B	0,63	0,10	0,35	-0,14
Turkey	F	1,86	0,95	1,34	1,18
South Korea	G	0,70	0,50	0,23	0,04
Russia	H	0,30	0,20	-1,30	-0,98
China	J	1,10	1,00	0,51	0,40

Table 19: Measurements of the *max profile deviation of the local radius from the least square mean radius value* related to the *indenter #122*.

Country	NMI code	NMI mean value (µm)	NMI exp. unc. (µm)	*E*n.w	*E*n.p
USA	B	0,47	0,10	-0,20	-0,67
Turkey	F	2,06	0,82	1,89	1,39
South Korea	G	0,60	0,50	0,20	-0,25
Russia	H	0,40	0,40	-0,24	-0,62
China	J	1,10	1,00	0,60	0,31

Table 20: Measurements of the *max profile deviation of the local radius from the least square mean radius value* related to the *indenter #130*.

Country	NMI code	NMI mean value (µm)	NMI exp. unc. (µm)	*E*n.w	*E*n.p
USA	B	0,30	0,10	-0,20	-0,53
Turkey	F	1,46	1,07	1,05	0,88
South Korea	G	0,30	0,50	-0,05	-0,29
Russia	H	0,50	0,40	0,42	0,05
China	J	1,10	1,00	0,77	0,60

11.2.4 Results of mean, expanded uncertainty and *E*n of straightness of the generatrix

Table 21: Measurements of the *straightness of the generatrix of the diamond cone* related to the *indenter #104*.

Country	NMI code	NMI mean value (µm)	NMI exp. unc. (µm)	*E*n.w	*E*n.p
Brazil	A	0,30	0,20	-2,17	-0,61
USA	B	0,91	0,05	2,53	0,96
Italy	D	0,30	0,15	-2,84	-0,64
Turkey	F	0,31	0,22	-1,93	-0,57
South Korea	G	1,00	0,50	0,51	0,72
Russia	H	0,18	0,14	-3,85	-0,95
China	J	1,50	1,00	0,76	0,89

Table 22: Measurements of the *straightness of the generatrix of the diamond cone* related to the *indenter #122*.

Country	NMI code	NMI mean value (µm)	NMI exp. unc. (µm)	*E*n.w	*E*n.p
Brazil	A	0,30	0,15	-3,59	-0,51
USA	B	1,10	0,05	3,69	1,26
Italy	D	0,30	0,15	-3,59	-0,51
Turkey	F	0,32	0,22	-2,41	-0,45
South Korea	G	0,70	0,50	-0,32	0,24
Russia	H	0,17	0,14	-4,71	-0,80
China	J	1,20	1,00	0,34	0,60

Table 23: Measurements of the *straightness of the generatrix of the diamond cone* related to the *indenter #130*.

Country	NMI code	NMI mean value (°)	NMI exp. unc. (°)	*E*n.w	*E*n.p
Brazil	A	0,30	0,15	-2,90	-0,99
USA	B	0,87	0,05	1,77	0,82
Italy	D	0,30	0,15	-2,90	-0,99
Turkey	F	0,51	0,22	-1,08	-0,32
South Korea	G	1,00	0,50	0,49	0,65
Russia	H	0,46	0,28	-1,03	-0,41
China	J	1,80	1,00	1,05	1,13

11.2.5 Results of mean, expanded uncertainty and *E*n of angle between the axes

Table 24: Measurements of the *angle between the axis of the diamond cone and the axis normal to the seating surface* related to the *indenter #104*.

Country	NMI code	NMI mean value (°)	NMI exp. unc. (°)	*E*n.w	*E*n.p
Brazil	A	0,06	0,04	-1,02	-0,72
USA	B	0,10	0,03	-0,28	-0,39
Italy	D	0,08	0,05	-0,48	-0,51
Germany	E	0,01	0,04	-2,23	-1,25
Turkey	F	0,05	0,06	-0,90	-0,76
South Korea	G	0,60	0,05	9,73	4,58
Russia	H	0,06	0,02	-2,01	-0,79
China	J	0,11	0,01	0,32	-0,24

Table 25: Measurements of the *angle between the axis of the diamond cone and the axis normal to the seating surface* related to the *indenter #122*.

Country	NMI code	NMI mean value (°)	NMI exp. unc. (°)	*E*n.w	*E*n.p
Brazil	A	0,03	0,04	-2,40	-1,17
USA	B	0,26	0,04	3,27	0,90
Italy	D	0,13	0,05	-0,07	-0,29
Germany	E	0,01	0,04	-2,90	-1,40
Turkey	F	0,14	0,06	0,11	-0,20
South Korea	G	0,51	0,05	7,28	2,98
Russia	H	0,09	0,02	-1,81	-0,69
China	J	0,14	0,08	0,08	-0,18

Table 26: Measurements of the *angle between the axis of the diamond cone and the axis normal to the seating surface* related to the *indenter #130*.

Country	NMI code	NMI mean value (°)	NMI exp. unc. (°)	*E*n.w	*E*n.p
Brazil	A	0,05	0,04	-1,45	-0,89
USA	B	0,19	0,03	2,16	0,35
Italy	D	0,09	0,05	-0,41	-0,51
Germany	E	0,03	0,04	-1,79	-1,04
Turkey	F	0,12	0,06	0,10	-0,27
South Korea	G	0,53	0,05	8,11	3,30
Russia	H	0,05	0,02	-2,56	-0,93
China	J	0,14	0,08	0,36	-0,07

11.2.6 Results of the weighted mean and Possolo weighted mean values and theirs expanded uncertainties calculated for the indenter geometric parameters

Table 27: Weighted mean values of the indenters for all geometric parameters considered.

	Indenter #104		Indenter #122		Indenter #130	
Parameter	Weighted mean	Expanded uncertainty	Weighted mean	Expanded uncertainty	Weighted mean	Expanded uncertainty
Cone angle	119,95	0,01	119,99	0,01	120,02	0,01
Tip Radius	198,41	0,43	202,17	0,41	204,86	0,37
Max profile	0,58	0,09	0,50	0,09	0,33	0,09
Straightness	0,74	0,04	0,86	0,04	0,75	0,04
Angle between axes	0,10	0,01	0,13	0,01	0,11	0,01

Table 28: Possolo weighted mean values of the indenters for all geometric parameters considered.

	Indenter #104		Indenter #122		Indenter #130	
Parameter	Possolo w. mean	Expanded uncertainty	Possolo w. mean	Expanded uncertainty	Possolo w. mean	Expanded uncertainty
Cone angle	119,96	0,03	119,99	0,03	120,02	0,04
Tip Radius	198,61	0,63	202,51	0,83	205,78	1,12
Max profile	0,68	0,33	0,77	0,43	0,47	0,31
Straightness	0,56	0,37	0,54	0,44	0,63	0,29
Angle between axes	0,13	0,09	0,16	0,11	0,15	0,10

11.3 Graphs of the mean values and their respective expanded uncertainties related to the NMI participants

The graphics analysis of the results obtained by the NMIs participants of this indenter pilot study are presented below. They are related to the geometric parameters listed on the technical protocol.

Additionally to the necessary dispersion analysis of the results between NMIs, the reference ISO tolerances were also considered, even not being so relevant is this particular pilot study.

11.3.1 Results of the mean value measurements of the included cone angle performed by the NMI participants for the indenters #104, #122 and #130

The NMIs measurement results related to the geometric parameter “included cone angle” are shown graphically from Figure 6 to Figure 8 for the three measurands. The data shows that the dispersion of all NMI results were small considering the weighted mean value and the Possolo weighted mean value, for all of the three indenters measured.

Beyond that, it should be noted that almost all NMI measurement results, with the exception of the NMI G, would have indicated that the included cone angles of the indenters #104 and #122 are within the maximum allowed tolerances specified for this parameter by the ISO 6508-3:2005 reference standard, as described in the clause 9 of this report. For the indenter #130, no NMI came outside of the Standard tolerances.

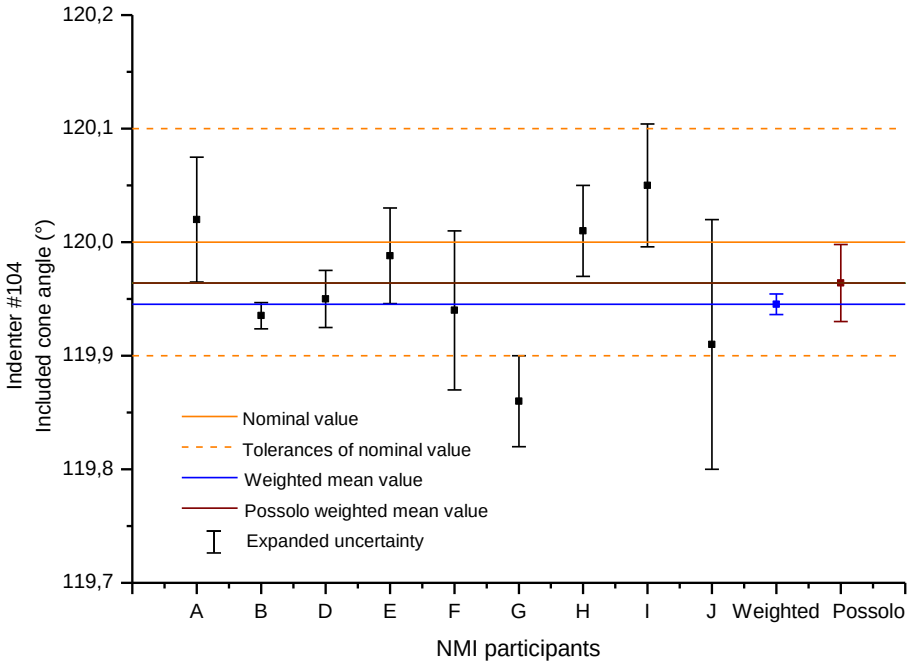

Figure 6: Mean values/error bars of the included cone angle obtained by the NMI participants, related to the indenter #104.

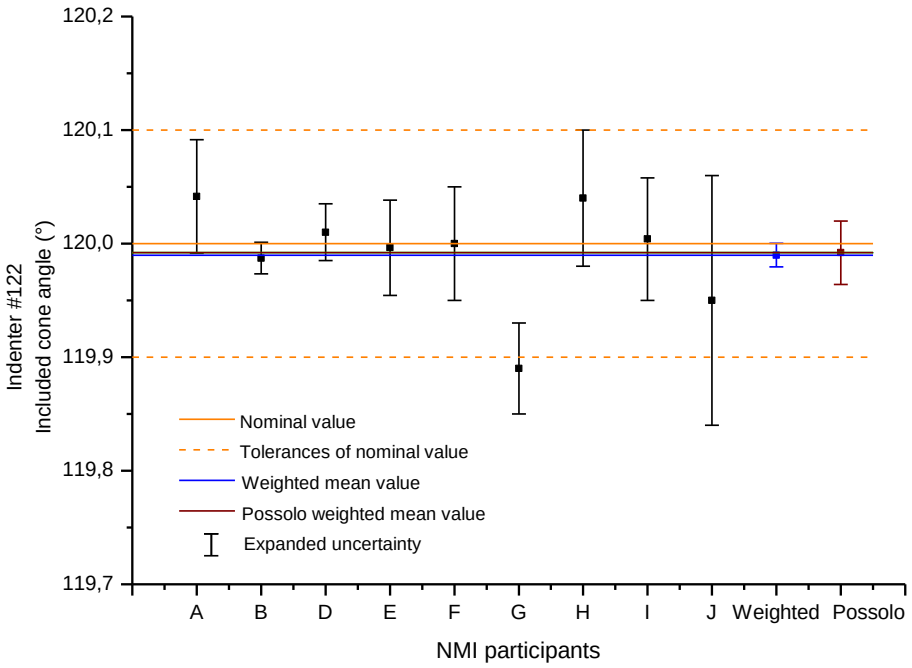

Figure 7: Mean values/error bars of the included cone angle obtained by the NMI participants, related to the indenter #122.

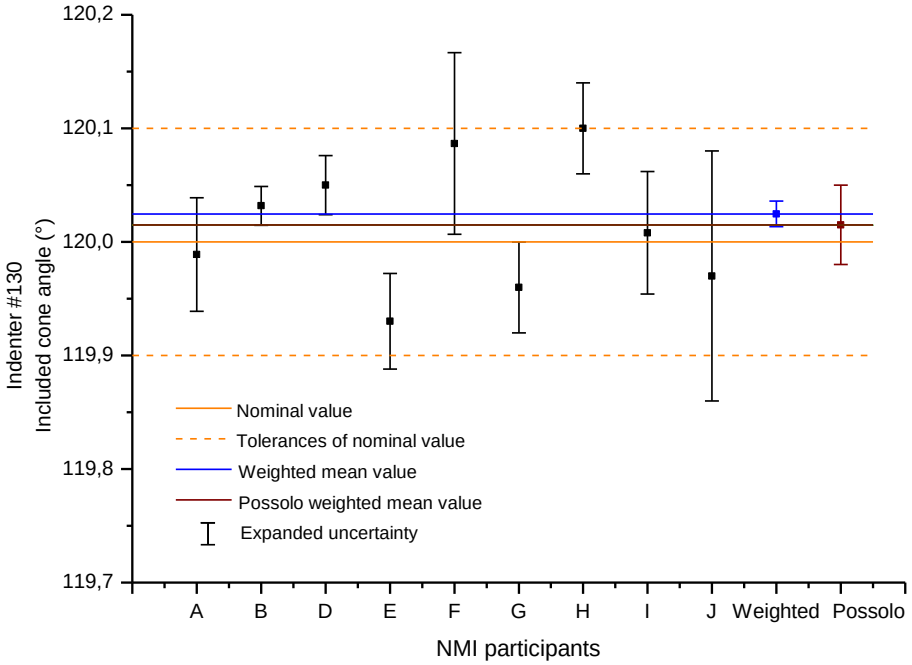

Figure 8: Mean values/error bars of the included cone angle obtained by the NMI participants, related to the indenter #130.

11.3.2.a Results of the mean values of the radius of the spherical tip performed by the NMI participants for the indenter #104

Figure 9 presents the data related to the geometric parameter “radius of the spherical tip” for the indenter #104. It is possible to see on it the good dispersion among the obtained results.

In this case, all NMIs results came inside the standard tolerances, as established in clause 9 of this report, noting however, the very large error bar, due to the expanded uncertainty, provided by the NMI E. It is also possible to see that the weighted mean value and the Possolo weighted mean value stayed a little far below to the nominal value (standard reference value).

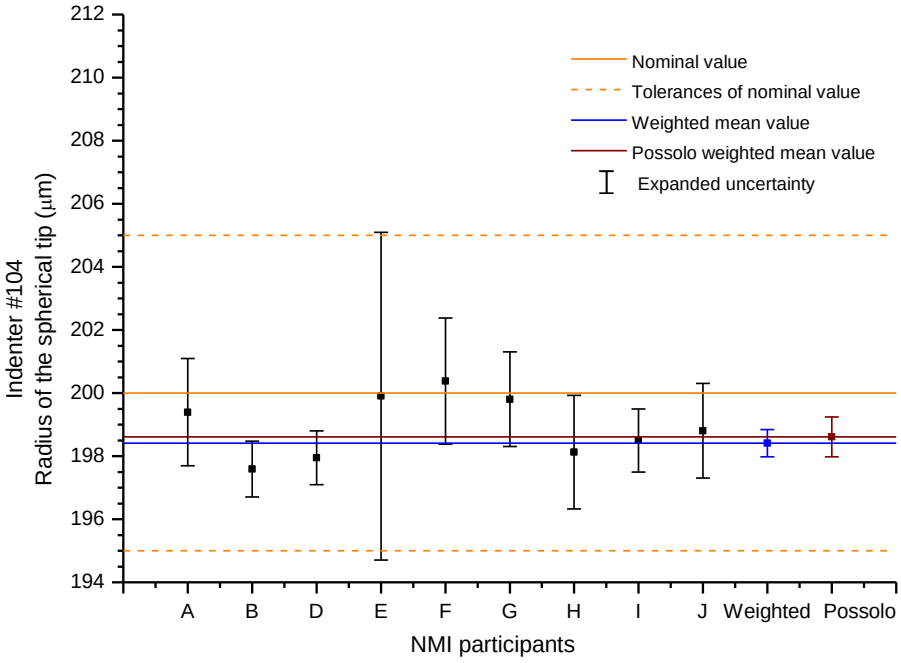

Figure 9: Mean values/error bars of the radius of the spherical tip obtained by the NMI participants, related to the indenter #104.

11.3.2.b Results of the mean values of the radius of the spherical tip performed by the NMI participants for the indenter #122

Figure 10 presents the graphic related to the geometric parameter “radius of the spherical tip” for the indenter #122. It is possible to observe in this figure a similarity with the indenter #104 in terms of dispersion among the majority of the NMIs results. However, while the weighted mean value and the Possolo weighted mean value of the indenter #104 stayed below to the nominal value (standard reference value), for the indenter #122, these average values stayed above it. In general, in this case, the error bars were similar.

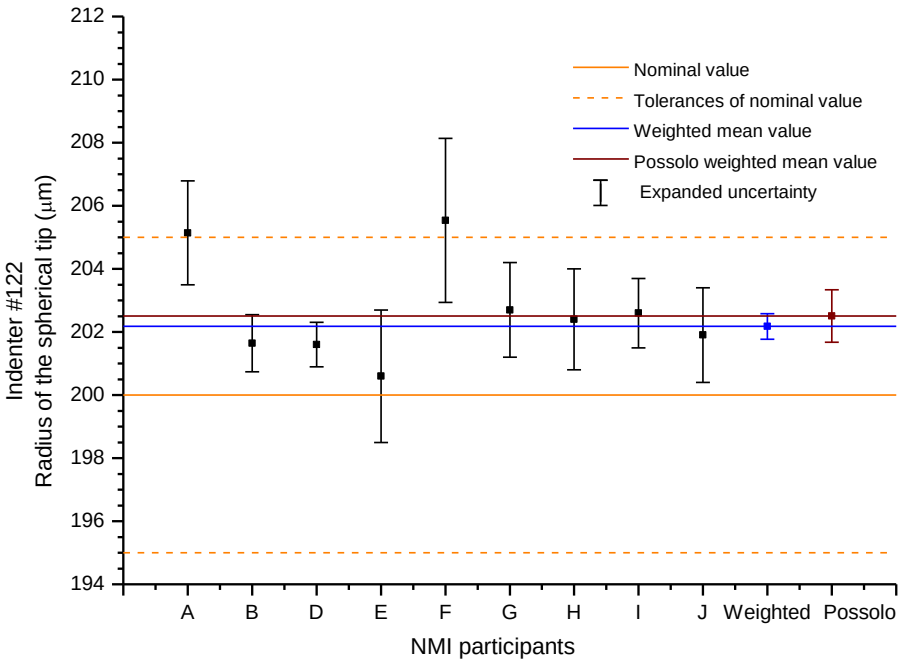

Figure 10: Mean values/error bars of the radius of the spherical tip obtained by the NMI participants, related to the indenter #122.

11.3.2.c Results of the mean values of the radius of the spherical tip performed by the NMI participants for the indenter #130

Figure 11 presents the graphic related to the geometric parameter “radius of the spherical tip” for the indenter #130. It is possible to see in this graphic a very good convergent among the results gave by the NMIs participants.

Having in mind the tolerances of the reference standard, all NMIs results as well as the average mean values stayed outside and very far above the higher tolerance.

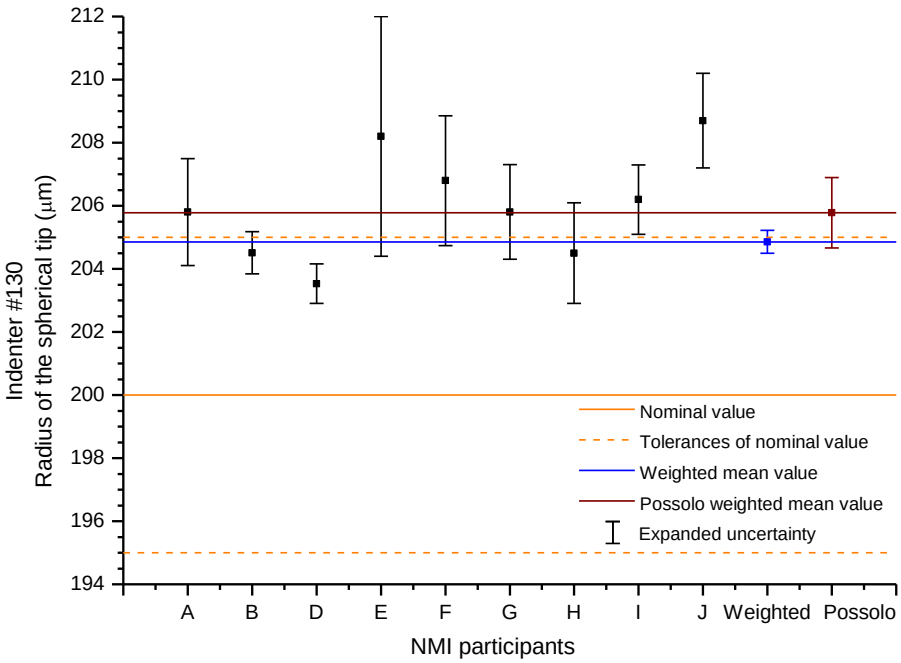

Figure 11: Mean values/error bars of the radius of the spherical tip obtained by the NMI participants, related to the indenter #130.

11.3.3 Results of the mean values of the max profile deviation of the radius from the true radius performed by the NMI participants for the indenters #104, #122 and #130

From Figure 12 to Figure 14 are presented the graphics related to the geometric parameter “max profile deviation” for the indenters #104, #122 and #130. It is possible to see that, with the exception of the NMI F for the indenter #122, all other measurements performed by the NMIs came inside the tolerance for this parameter, as described in the clause 9 of this report. Is it also important to point out that, the NMIs F and J presented very large expanded uncertainties for this parameter, as shown by the error bars.

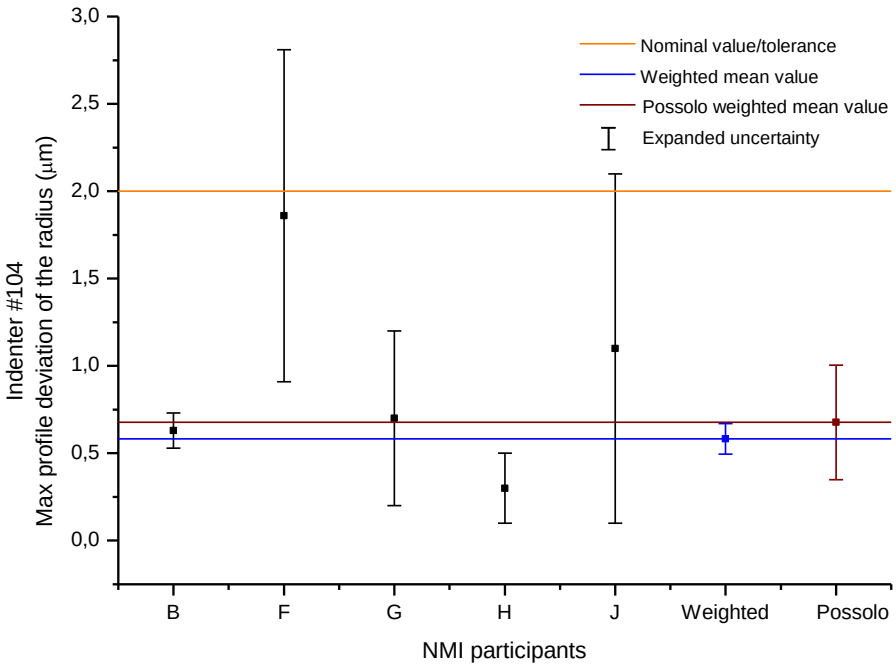

Figure 12: Mean values/error bars of the max profile deviation of the radius from a true radius obtained by the NMI participants, related to the indenter #104.

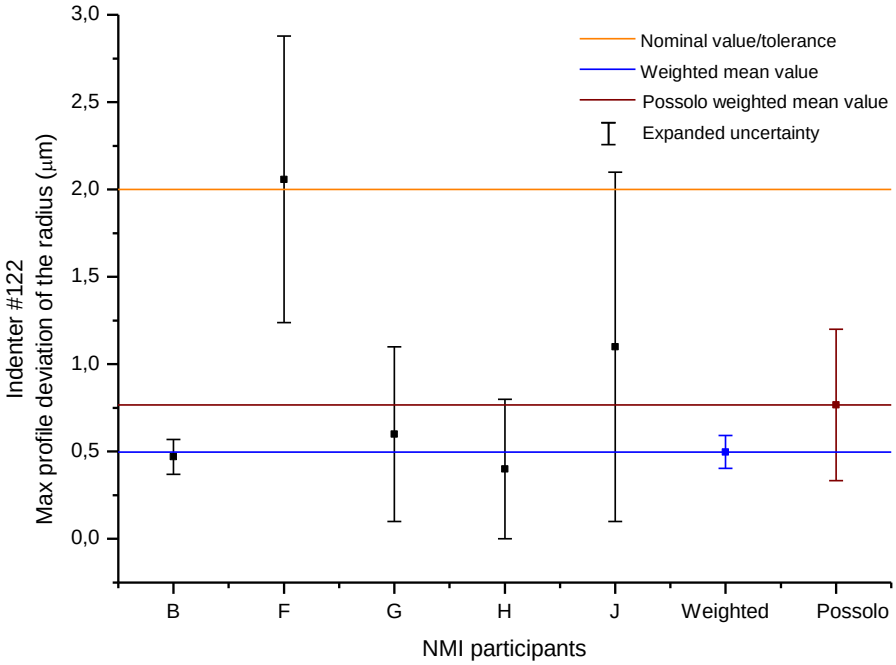

Figure 13: Mean values/error bars of the max profile deviation of the radius from a true radius obtained by the NMI participants, related to the indenter #122.

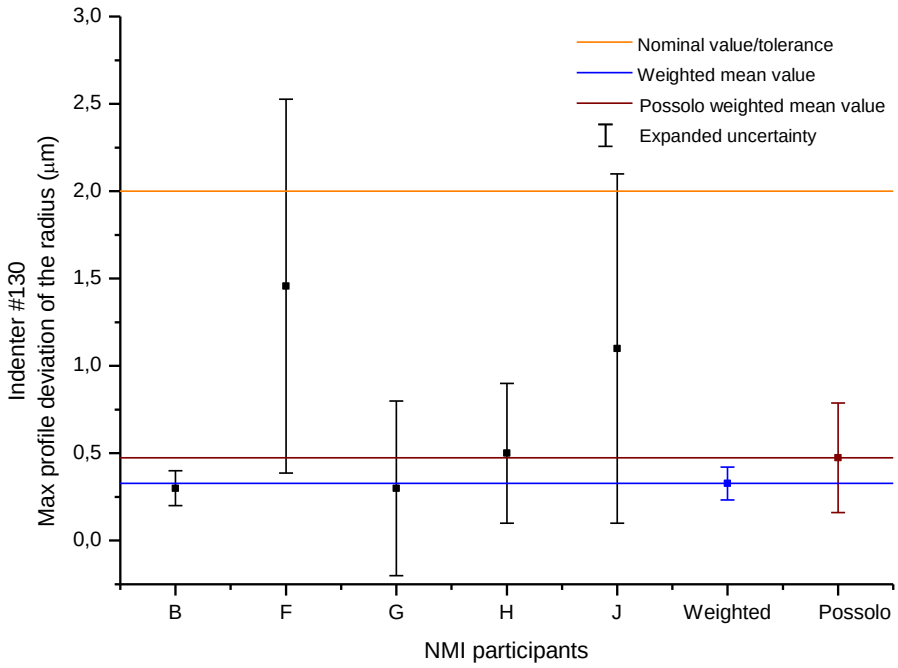

Figure 14: Mean values/error bars of the max profile deviation of the radius from a true radius obtained by the NMI participants, related to the indenter #130.

11.3.4 Results of the mean values of the straightness of the generatrix of the diamond cone performed by the NMI participants for the indenter #104, #122 and #130

Figures 15, 16 and 17 presents the graphics related to the geometric parameter "straightness of the generatrix" for the indenter #104, #122 and #130. It is possible to notice in these figures the similarity of the obtained results, as well as the dispersions, from the NMIs A, D, F and H.

It is also possible to see that the weighted mean value and the Possolo weighted mean value stayed outside/above to the nominal values (standard reference value), probably due to the higher values provided by the NMIs B, G and J, which stayed far from the tolerance limits. The largest error bars in these figures were due to the NMIs G and J.

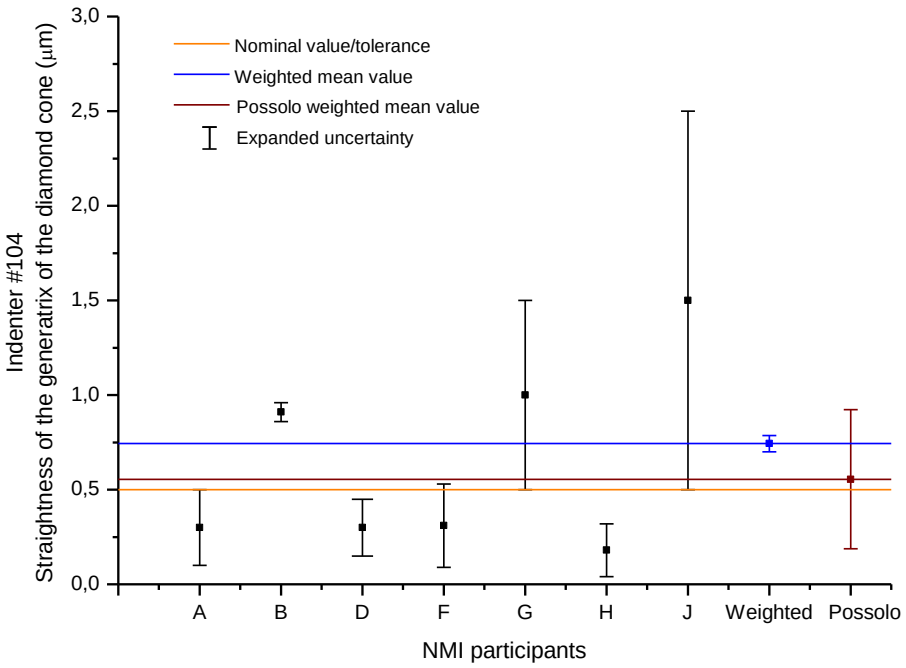

Figure 15: Mean values/error bars of the straightness of the generatrix of the diamond cone obtained by the NMI participants, related to the indenter #104.

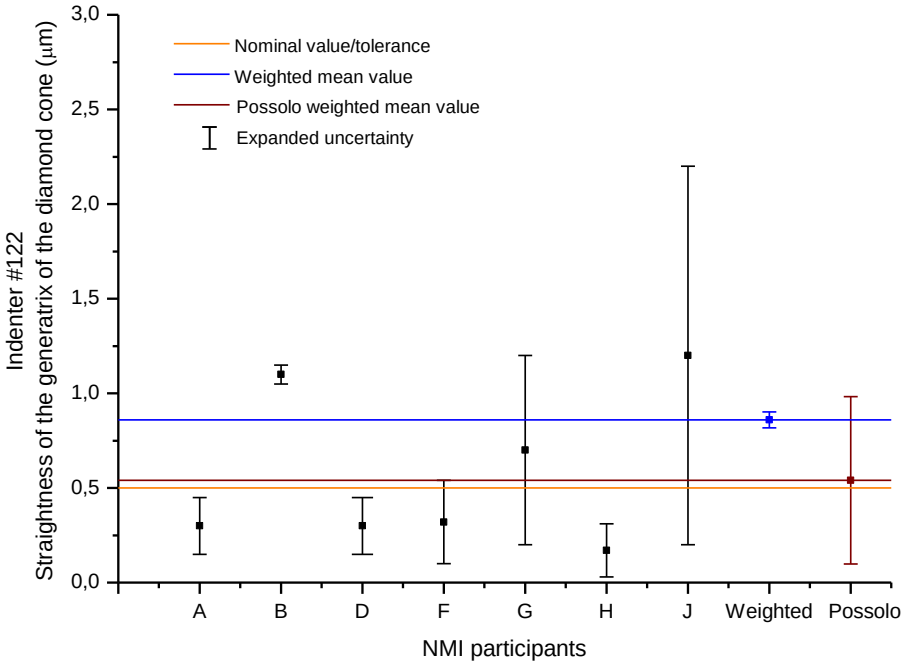

Figure 16: Mean values/error bars of the straightness of the generatrix of the diamond cone obtained by the NMI participants, related to the indenter #122.

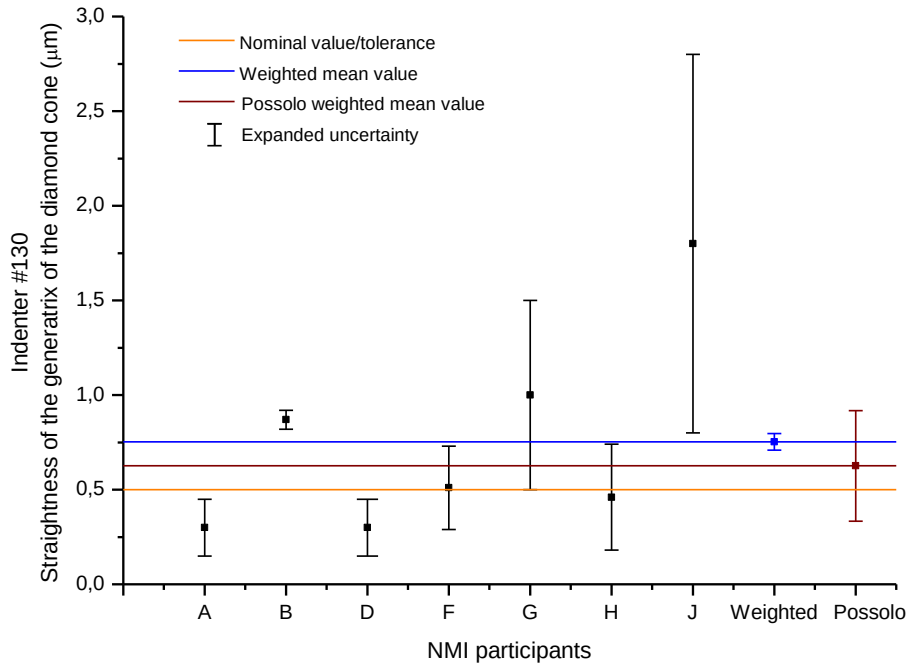

Figure 17: Mean values/error bars of the straightness of the generatrix of the diamond cone obtained by the NMI participants, related to the indenter #130.

11.3.5 Results of the mean values of the angle between the axis of the diamond cone and the axis normal to the seating surface performed by the NMI participants for the indenters #104, #122 and #130

From Figure 18 to Figure 20 are presented the graphics related to the geometric parameter “angle between axes” for the indenters #104, #122 and #130. It is possible to see in these graphics that, with the exception of NMI G, all other NMIs stayed around the average values and inside the limit pre-established in clause 9 of this report. Besides, the NMI G stayed very far beyond the mean values and consequently, outside the acceptable limit.

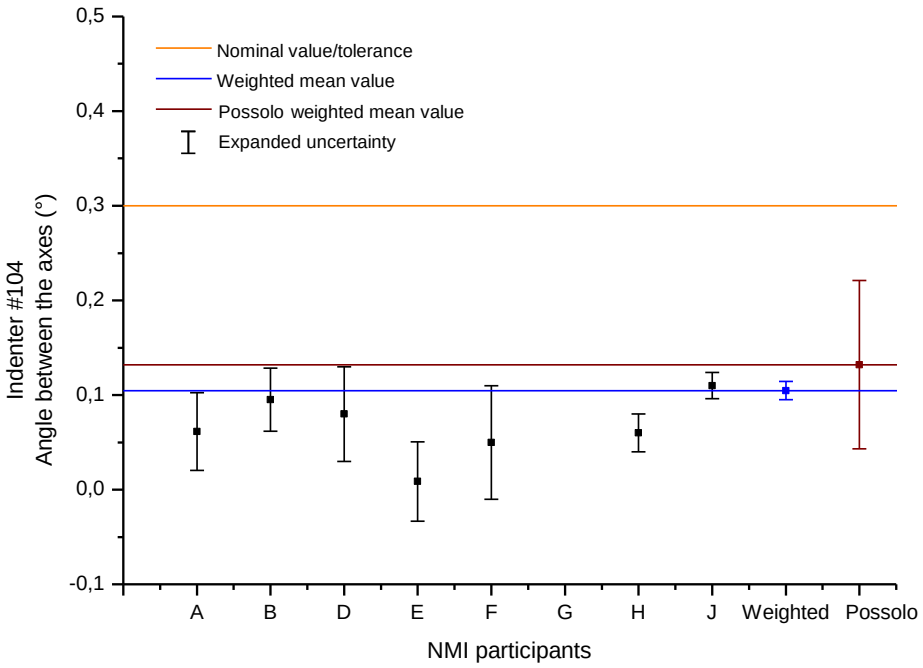

Figure 18: Mean values/error bars of the angle between the axis of the diamond cone and the axis normal to the seating surface obtained by the NMI participants, related to the indenter #104.

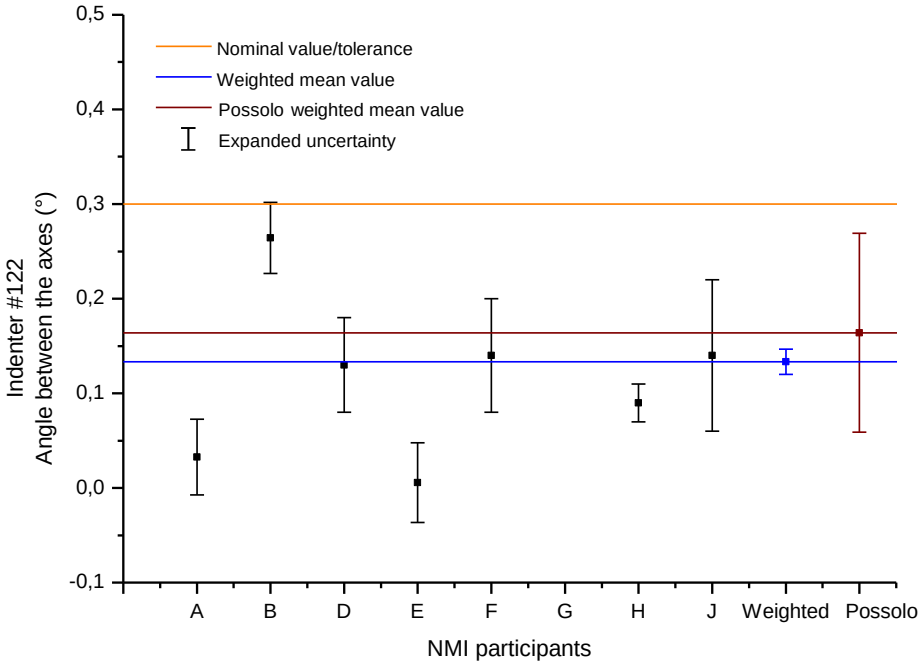

Figure 19: Mean values/error bars of the angle between the axis of the diamond cone and the axis normal to the seating surface obtained by the NMI participants, related to the indenter #122.

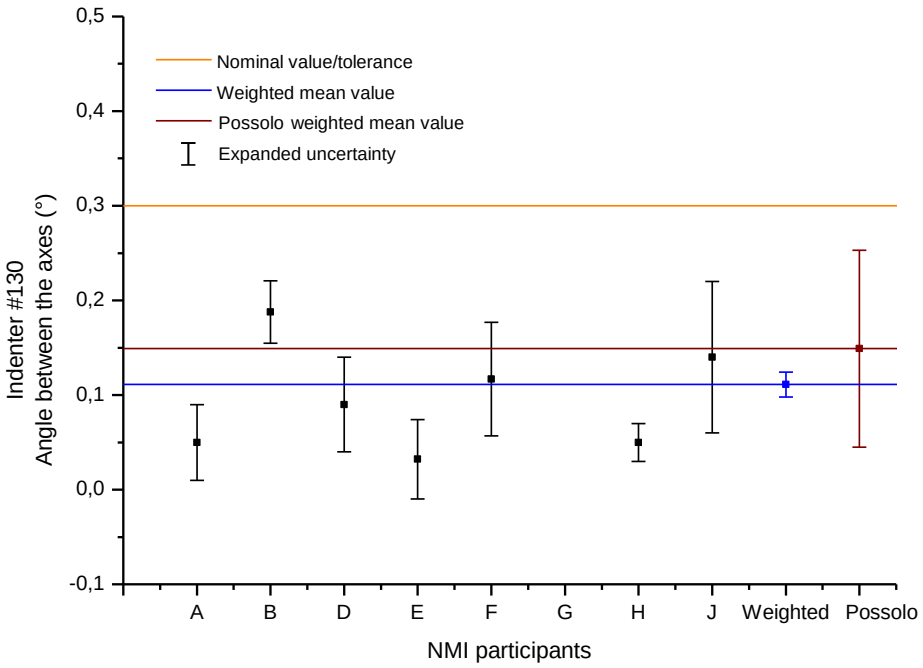

Figure 20: Mean values/error bars of the angle between the axis of the diamond cone and the axis normal to the seating surface obtained by the NMI participants, related to the indenter #130.

11.4 Graphs of the calculated *E*n related to the NMI participants

The following graphics are presenting the *E*n calculated for all NMIs related to the geometric parameters considered in this pilot study. As described in clause 10, two methods of calculation were done. One from the weighted mean (*E*n.w) and other from the Possolo weighted mean (*E*n.p).

11.4.1 Indenters #104, #122 and #130 "included cone angle"

The behavior of *E*n, calculated for all NMIs related to the parameter included cone angle, is described in the Figures 21, 22 and 23. It is possible to see in these figures the influence caused by the different methods of analysis, where some NMIs stayed inside the En limits and others not, depending on the method considered, e.g., NMIs A and H for the indenter #104.

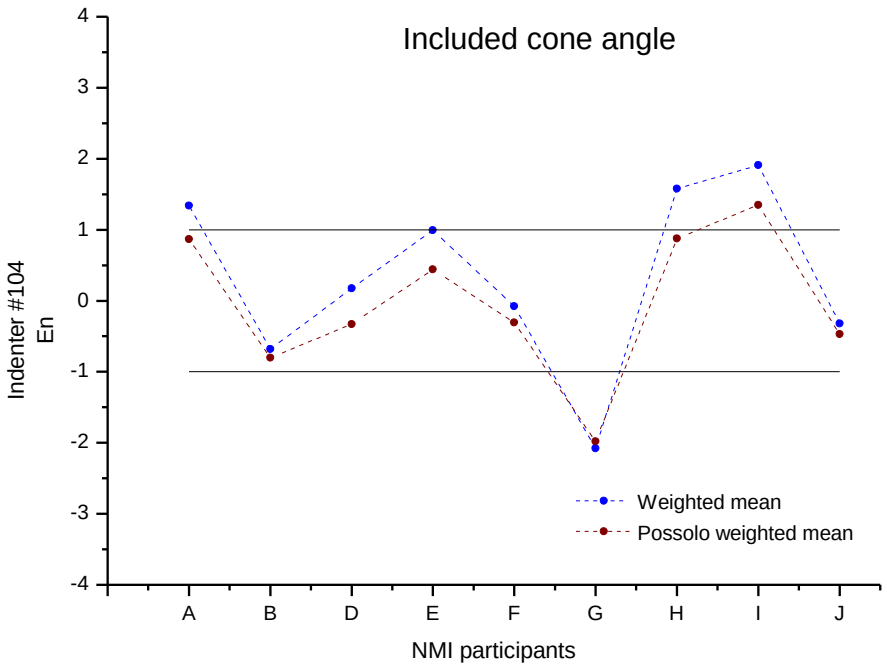

Figure 21: *E*n calculated for the NMI participants, related to the included cone angle of the indenter #104.

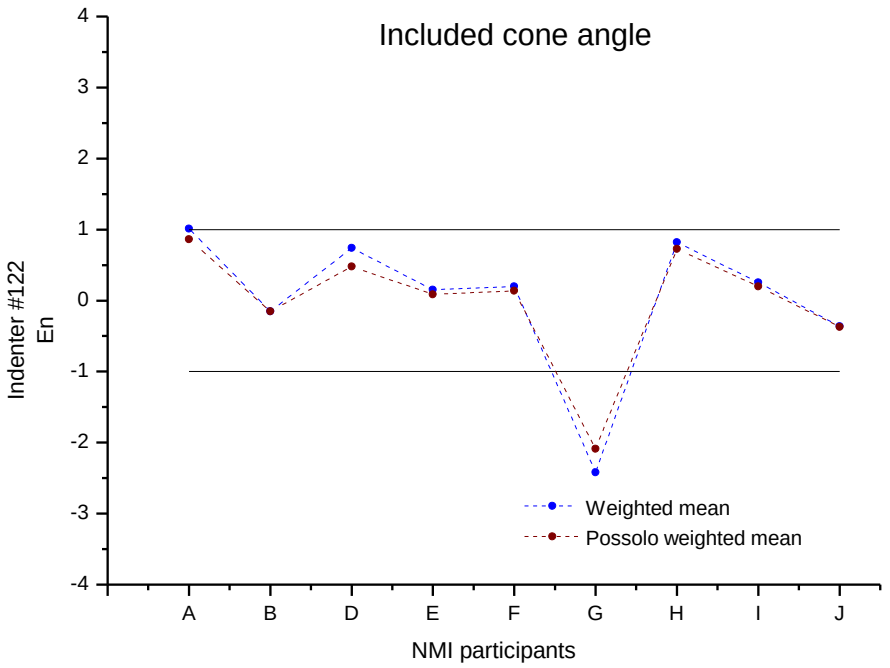

Figure 22: *E*n calculated for the NMI participants, related to the included cone angle of the indenter #122.

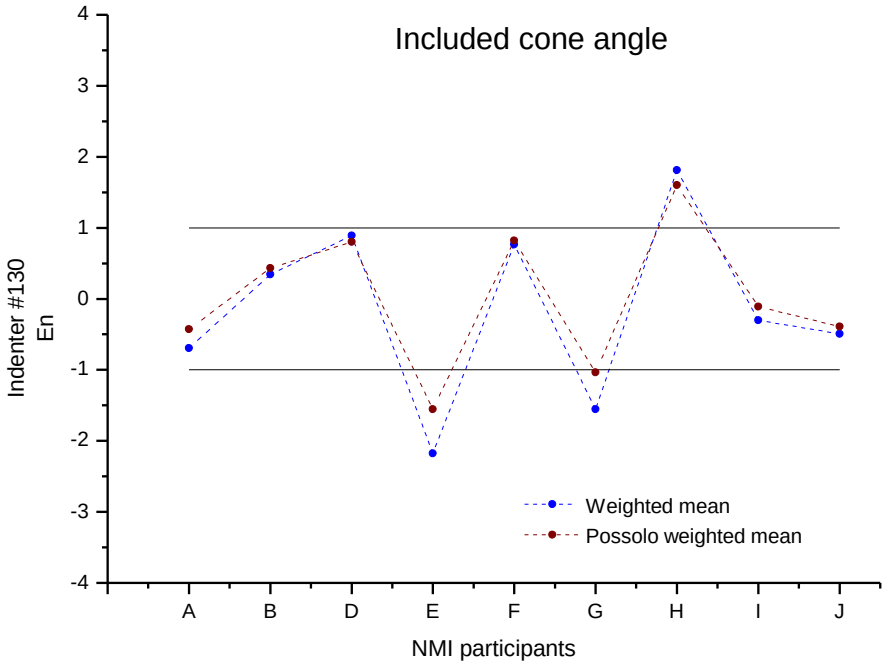

Figure 23: *E*n calculated for the NMI participants, related to the included cone angle of the indenter #130.

11.4.2 Indenters #104, #122 and #130 “radius of the spherical tip”

The Figures 24 and 25 are related to *E*n calculated to the indenters #104 and #122. In these figures is possible to see the consistent results of all NMIs no matter the method of analysis considered. However, the Figure 26, related to the indenter #130 is showing that the NMI I is inside the *E*n tolerances for the Possolo weighted mean but outside the *E*n tolerances for the weighted mean values.

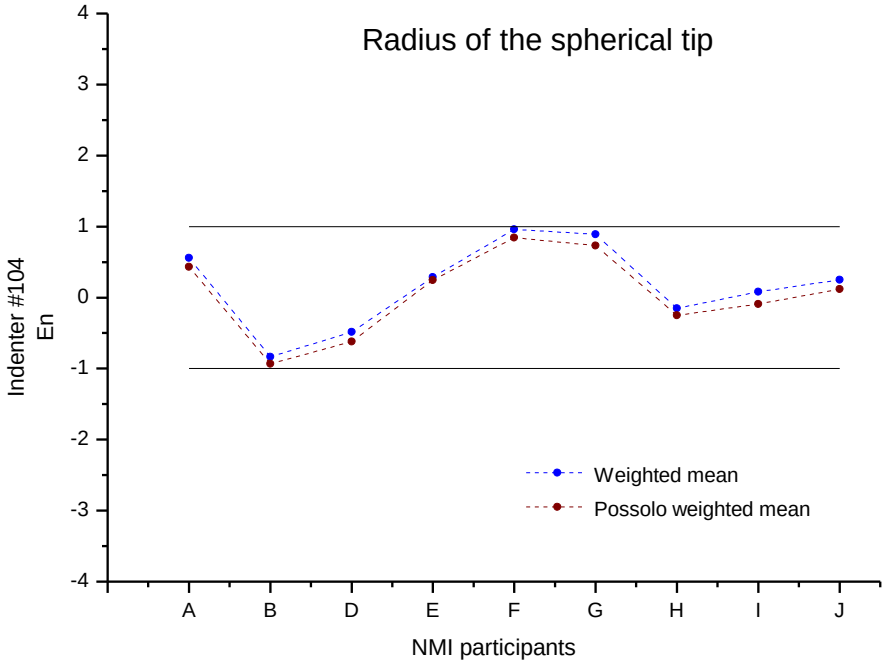

Figure 24: *E*n calculated for the NMI participants, related to the radius of the spherical tip of the indenter #104.

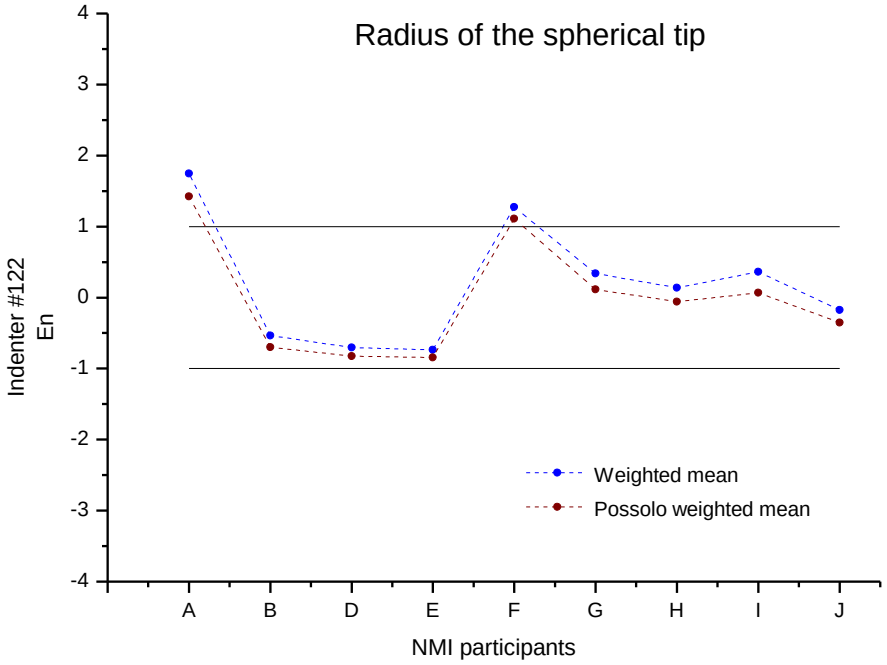

Figure 25: *E*n calculated for the NMI participants, related to the radius of the spherical tip of the indenter #122.

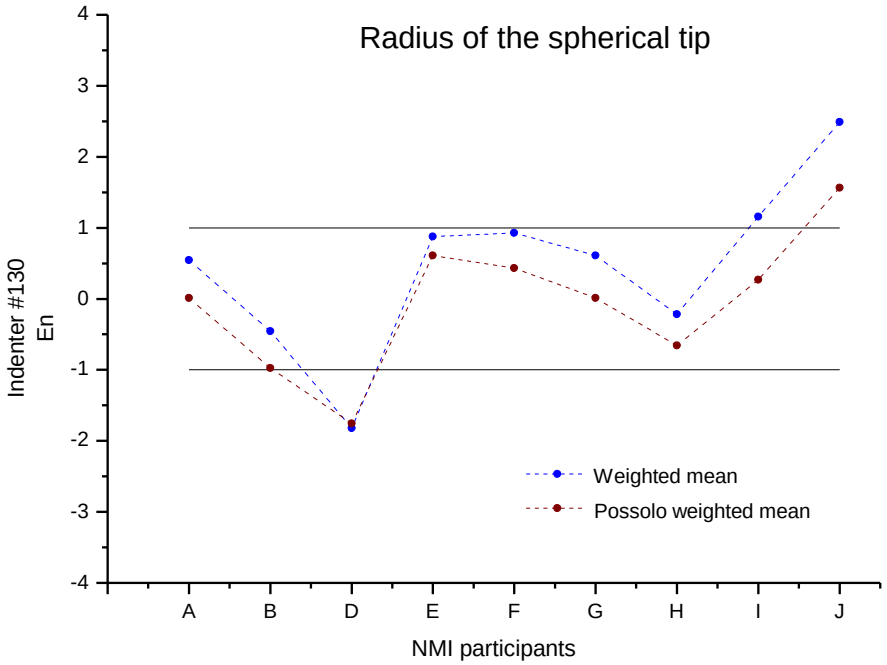

Figure 26: *E*n calculated for the NMI participants, related to the radius of the spherical tip of the indenter #130.

11.4.3 Indenters #104, #122 and #130 “Max profile deviation”

The following Figures 27, 28 and 29, related to the parameter max profile deviation of the radius are showing the behavior of *E*n, calculated for all NMIs. It is possible to see in these graphics that the NMI F came outside the *E*n tolerance for almost all indenters measured, with the exception for the measurement of the indenter #130, but only when the Possolo weighted mean method of analysis is considered.

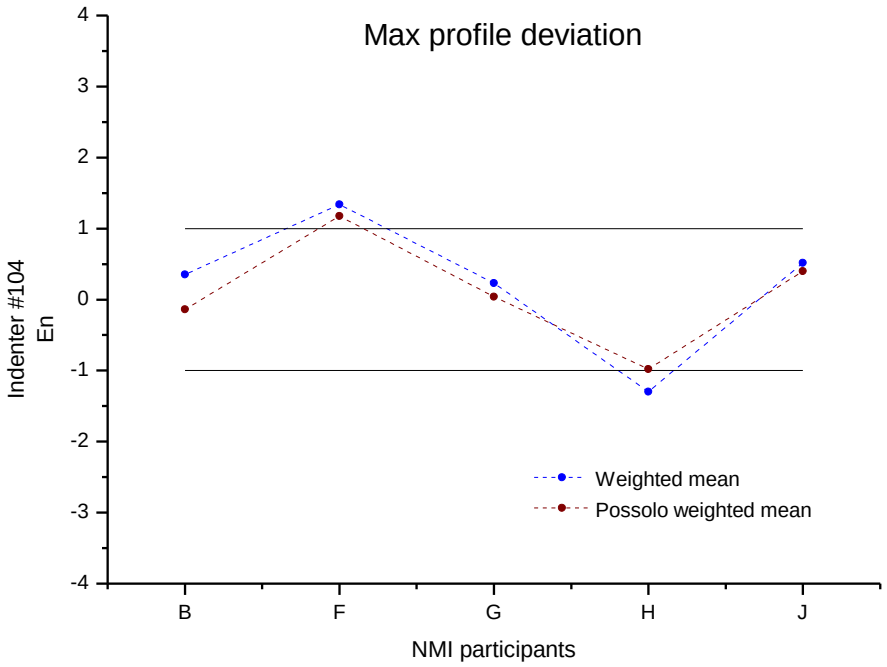

Figure 27: *E*n calculated for the NMI participants, related to the max profile deviation of the radius of the indenter #104.

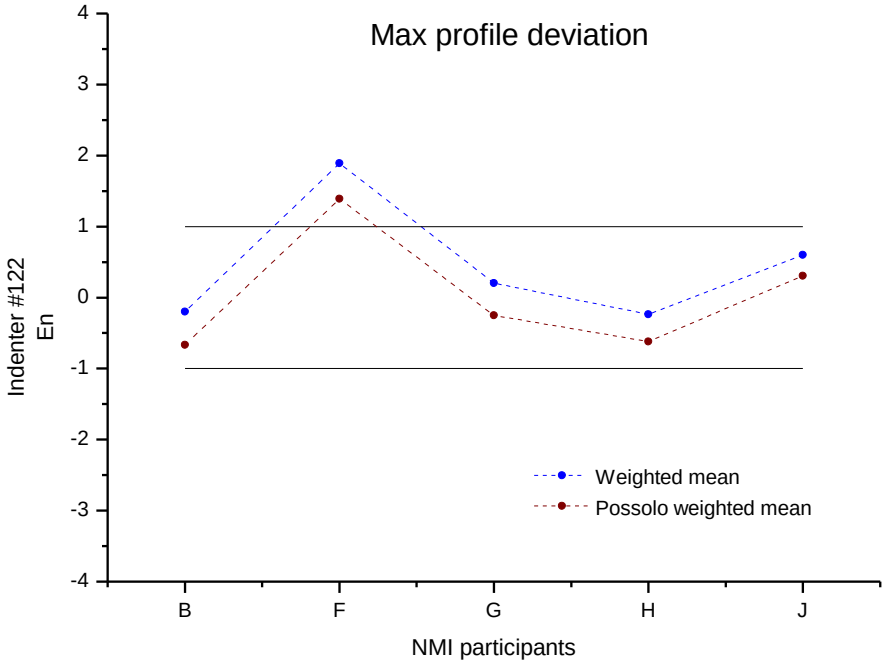

Figure 28: *E*n calculated for the NMI participants, related to the max profile deviation of the radius of the indenter #122.

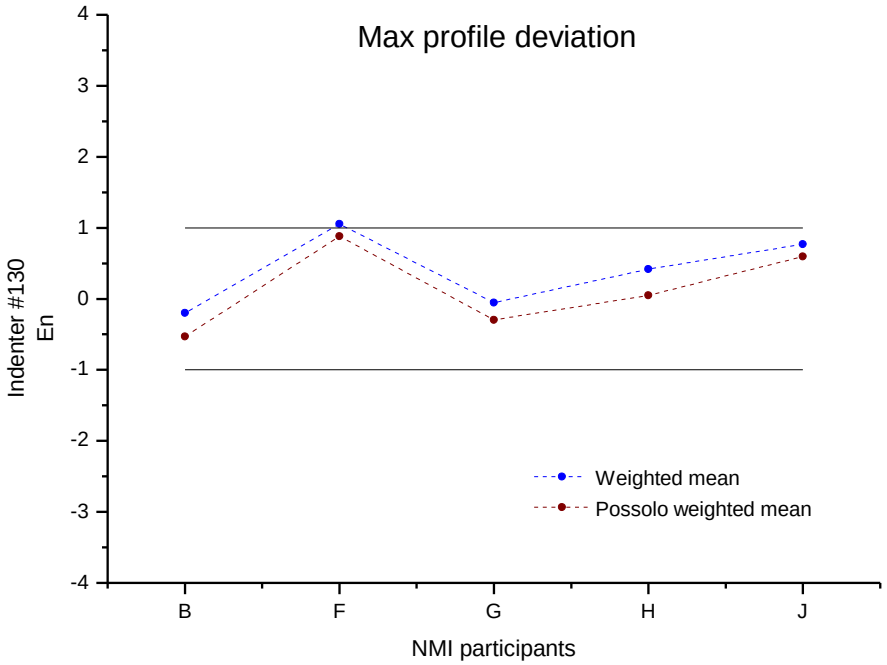

Figure 29: *E*n calculated for the NMI participants, related to the max profile deviation of the radius of the indenter #130.

11.4.4 Indenters #104, #122 and #130 “straightness of the generatrix”

In the Figures 30, 31 and 32, which are related to the parameter straightness of the generatrix of the diamond cone, is easy to see the dependence of *E*n behavior, calculated for all NMIs if one consider different method of analysis. The Possolo weighted mean method provided all *E*n results inside the acceptable tolerances. However, if one consider the weighted mean method, some or the majority of the NMIs came outside them, no matter the indenter measured.

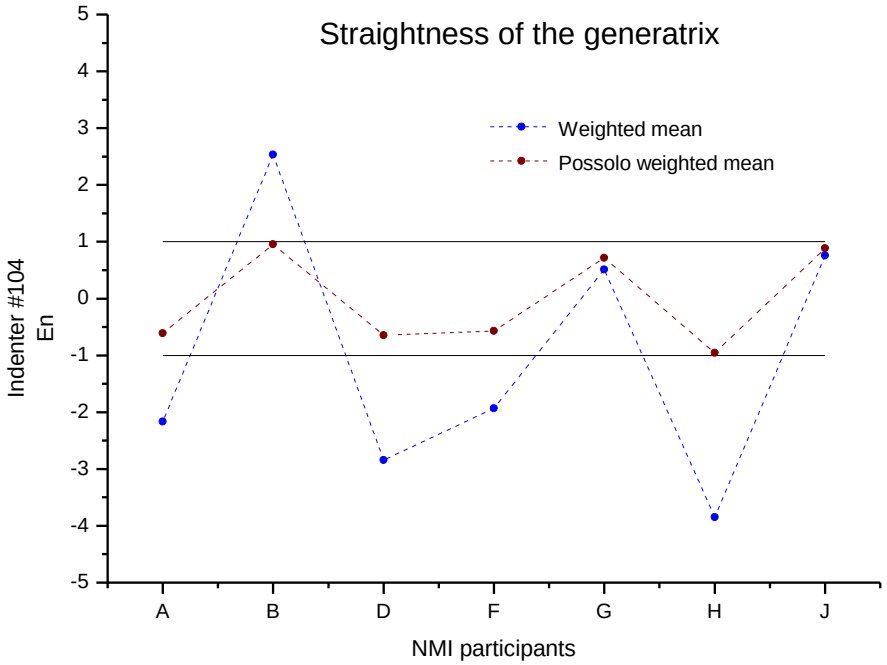

Figure 30: *E*n calculated for the NMI participants, related to the straightness of the generatrix of the diamond cone of the indenter #104.

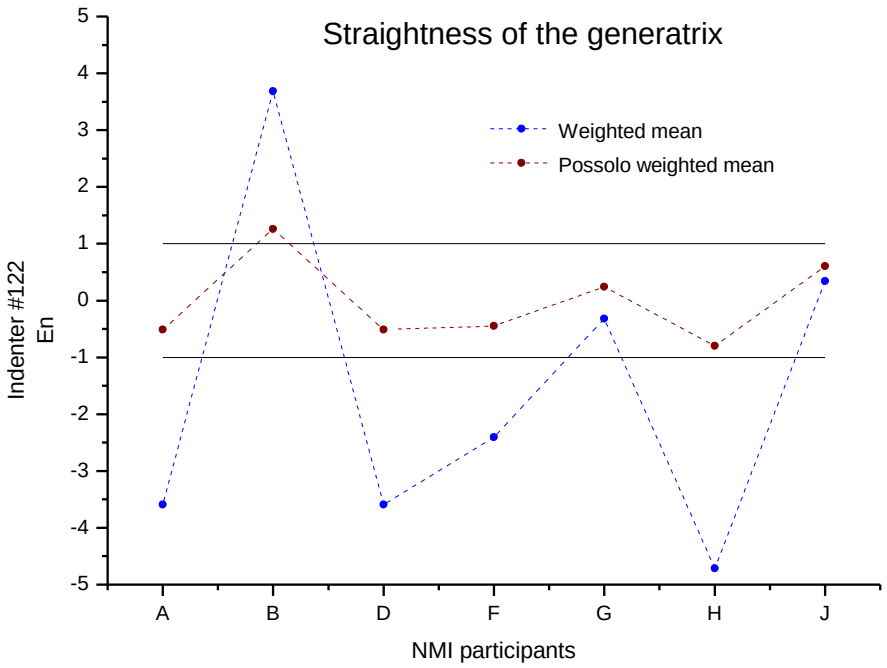

Figure 31: *E*n calculated for the NMI participants, related to the straightness of the generatrix of the diamond cone of the indenter #122.

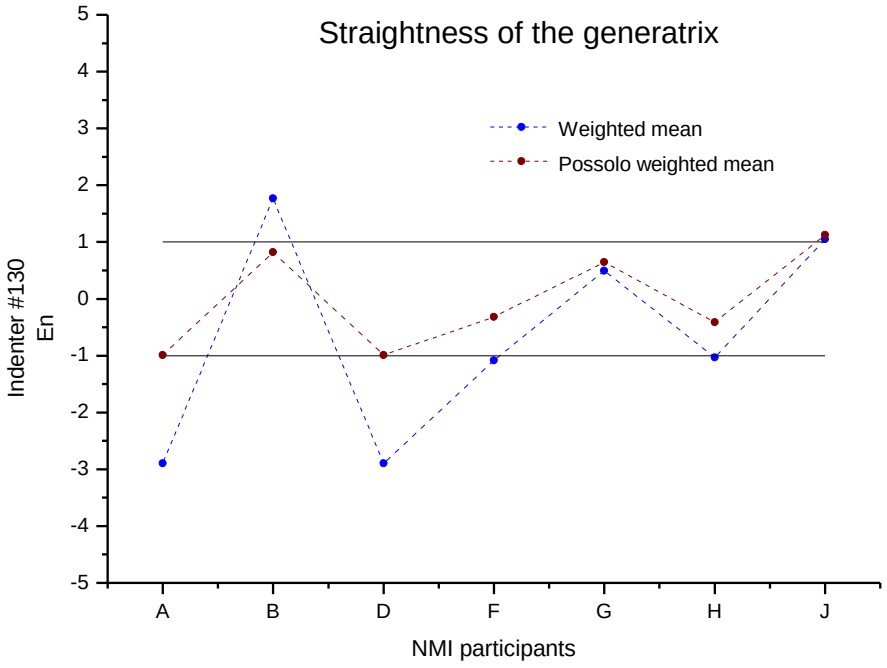

Figure 32: *E*n calculated for the NMI participants, related to the straightness of the generatrix of the diamond cone of the indenter #130.

11.4.5 Indenters #104, #122 and #130 “angle between axes”

It is very clear in the Figures 33, 34 and 35, that the behavior of *E*n calculated for the NMI G, for all indenters measured, came far above the top limit, while the other NMIs stayed closer to the limits. However, it is necessary to point out too that in some cases the method of analysis provided *E*n results where some NMIs came or inside or outside the *E*n limit for the same angle between axes measured for the same indenter.

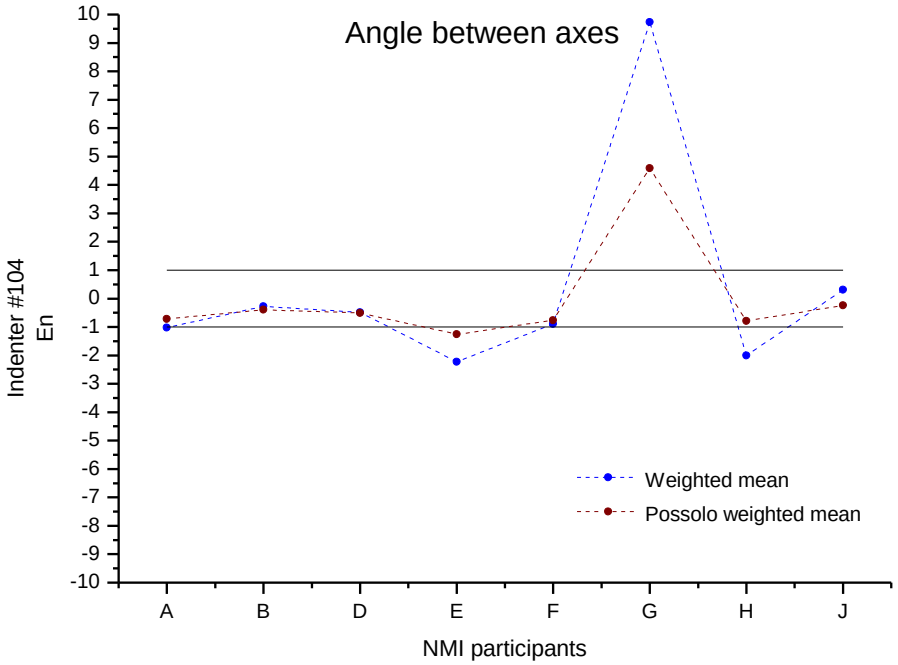

Figure 33: *E*n calculated for the NMI participants, related to the angle between the axis of the diamond cone and the axis normal to the seating surface of the indenter #104.

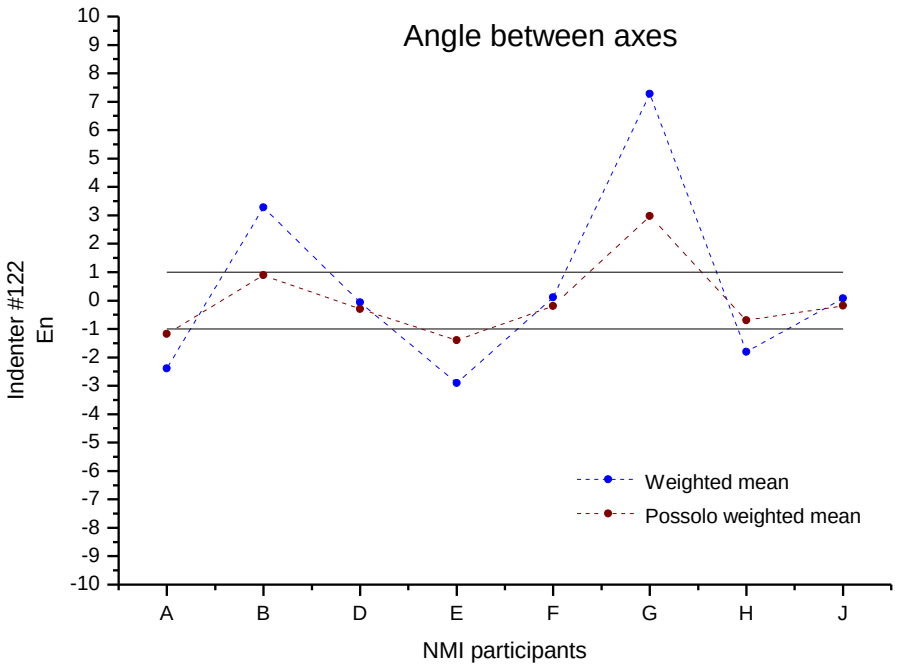

Figure 34: *E*n calculated for the NMI participants, related to the angle between the axis of the diamond cone and the axis normal to the seating surface of the indenter #122.

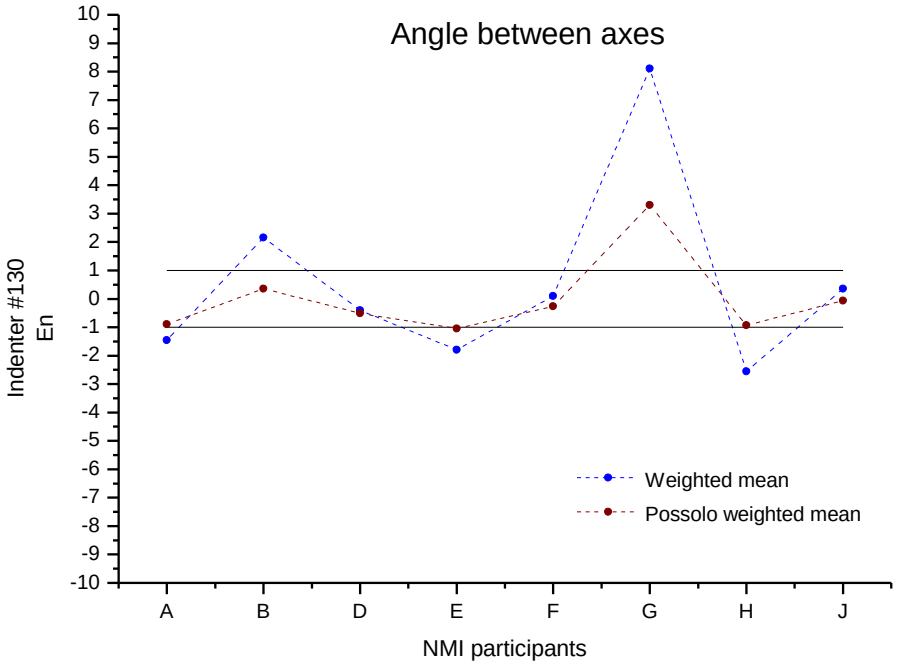

Figure 35: *E*n calculated for the NMI participants, related to the angle between the axis of the diamond cone and the axis normal to the seating surface of the indenter #130.

12. DISCUSSIONS

This comparison had nine participating labs from National Metrology Institutes, of Europe, Asia and Americas, where they had to measure the same geometric parameters of three indenters. However, no reference value and thus no uncertainty of a reference value were assigned. Each Lab obtained an average value of the same number of measurements, for each parameter, and reported the mean values with their respective measurement uncertainties.

Considering the plotted graphics (clause 11), this study may pointed out that either many (or all) the labs are underestimating their uncertainties, as all measurements are dealing with hardness, and/or they are not measuring exactly the same thing, if one, for example, consider different window sizes and areas for the radius, cone angle and / or cone straightness. This is because, the inclusion of only a tiny part of the radius-cone blend area in the measurement, can cause large measurement differences.

Additionally, it is necessary to consider the method of analysis used to calculate the normalized errors. The *weighted mean method* is one of the most used method in comparisons, which is based on the reproducibility between the Labs (standard deviation of the mean). However, it ignores the Labs reported measurement uncertainties.

Alternatively, the NICOB (Possolo weighted mean method) was also considered to calculate the normalized errors. This method is particularly appropriate when the measured values are more dispersed than expected to be in light of the reported uncertainties, which seems to be this comparison, where it is showing significant heterogeneity in the measured results.

REFERENCES

[1] ISO 6508-3:2005 Metallic materials - Rockwell hardness test - Part 3: Calibration of reference blocks (scales A, B, C, D, E, F, G, H, K, N, T), International Organisation for Standardisation, Geneva, Switzerland.

[2] J. F. Song, F. F. Rudder, Jr., T. V. Vorburger, and J. H. Smith. Microform Calibration Uncertainties of Rockwell Diamond Indenters. J. Res. Natl. Inst. Stand. Technol. 1995 Sep-Oct; 100(5): 543–561.

[3] ISO 6508-2:2005 Metallic materials - Rockwell hardness test - Part 2: Verification and calibration of testing machines (scales A, B, C, D, E, F, G, H, K, N, T), International Organisation for Standardisation, Geneva, Switzerland.

[4] ISO/IEC Guide 98-3:2008 Uncertainty of measurement - Part 3: Guide to the expression of uncertainty in measurement (GUM:1995).

[5] EURAMET cg-16 Version 2.0 (03/2011): Guidelines on the Estimation of Uncertainty in Hardness Measurements. European Association of National Metrology Institutes.

[6] John Song, Samuel Low and Alan Zheng. Geometric measurement comparisons for Rockwell diamond indenters. In: XIX IMEKO World Congress Fundamental and Applied Metrology. September 6−11, 2009, Lisbon, Portugal.

[7] Febo Menelao, Zhi Li, Uwe Brand and Andre Felgner. A non-imaging optical system for characterisation of ball-shaped micro-indenters. In: IMEKO 22nd TC3, 12th TC5 and 3rd TC22 International Conferences. 3 to 5 February, 2014, Cape Town, Republic of South Africa.

[8] NIST Consensus Builder User's Manual. Amanda Koepke, Thomas Lafarge, Antonio Possolo, Blaza Toman. Statistical Engineering Division Information Technology Laboratory. National Institute of Standards and Technology, Gaithersburg, MD, 2017.

[9] Amanda Koepke et al 2017 Metrologia 54 S34. https://doi.org/10.1088/1681-7575/aa6c0e

[10] J. Song, S. Low, A. Zheng and P. Gu. Geometrical measurements of NIST SRM Rockwell hardness diamond indenters. In: IMEKO 2010 TC3, TC5 and TC22 Conferences Metrology in Modern Context. November 22−25, 2010, Pattaya, Chonburi, Thailand.

[11] ASTM E18-07 Standard Test Method for Rockwell Hardness of Metallic Materials, American Society for Testing and Materials, Philadelphia, USA, 2007.

Annex A CCM.H-P1 registration on BIPM.KCDB@bipm.org

Key and supplementary comparisons (and pilot studies) - registration and progress form

Comparison conducted by CC **in** M	**Date: 03/07/2014**
1. Subfield: **Hardness**	RMO internal identifier
2. KCDB identifier: **CCM.H-P1** *(for KCs and SCs)* *(to be attributed by the BIPM)*	
3.Type of comparison: Key ☐ Supplementary ☐ Pilot study ☒	4. Short description: Pilot Study on the measurement of Rockwell hardness diamond indenters in which the hardness and/or dimensional metrology laboratories of National Metrology Institutes (NMIs) should
5. Measurand and nominal value(s): Included cone angle: 120° Spherical tip radius: 0.2 mm Straightness of the generatrix of the diamond cone over 0.4 mm: 0.0 mm	Special characters for copying *(if required)* α β Γ γ Δ δ ε ζ η θ ι κ λ μ
6. Parameter(s): Length, angle	
7. Transfer device(s)/sample(s): Three Rockwell hardness diamond indenters designated as indenters 104, 122 and 130	
8. Pilot laboratory(ies) *(acronyms and countries)*: INMETRO, Brazil	
9. Participating institutes *(acronyms and countries)*: INMETRO, Brazil; NIST/USA; INRiM/Italy; NPL/UK; PTB/Germany; UME/Turkey; KRISS/Republic of Korea; VNIIFTRI/Russia; NMIJ/Japan; NIM/PR China and NMIT/Thailand	

10. Progress: *(please note date and tick appropriate box to indicate current status)*

Date	Status	Pilot	Supplementary		Key
_____	Planned	☐	☐		☐
_____	Protocol complete	☐	☐		☐
_____	In progress	☐	☐		☐
_____	Measurement completed	☒	☐		☐
_____	Report in progress	☐	☐	Draft A	☐
				Draft B	☐
_____	Report submitted to _____	☐	☐		☐
_____	Results approved	☐	☐		
_____	Approved for equivalence				☐
_____	Abandoned	☐	☐		☐

Comments:	Publication reference:
11. Measurement start date: **12/2010**	12. (Expected) measurement completion date: _____
13. Contact person's name: Renato Reis Machado	
Address: Instituto Nacional de Metrologia, Qualidade e Tecnologia Av. N. Sra. das Graças, 50, Xerém Duque de Caxias, RJ 25250-020 Brazil	Tel.: **+55.21.2679.9050** Fax: **+55.21.2679.1505** e-mail: rrmachado@inmetro.gov.br Web: **www.inmetro.gov.br**

Completed copy to be forwarded to a) CCXX Executive Secretary;
b) relevant CC Key Comparison WG Chairman;
c) Regional coordinator as appropriate;
d) KCDB Coordinator (except Pilot studies): BIPM.KCDB@bipm.org